Journal of Solar Energy Science & Research

Volume No. 8

Issue No. 1

January - April 2024

ENRICHED PUBLICATIONS PVT. LTD

S-9, IInd FLOOR, MLU POCKET,
MANISH ABHINAV PLAZA-II, ABOVE FEDERAL BANK,
PLOT NO-5, SECTOR-5, DWARKA, NEW DELHI, INDIA-110075,
PHONE: - + (91)-(11)-47026006

Journal of Solar Energy Science & Research

Aims and Scope

The Journal of Solar Energy Science and Research is published quarterly by Enriched publications. Journal of Solar Energy Science and Research is peer reviewed journal and monitored by a team of reputed reviewers. Today, the journal continues to publish articles on topics ranging from solar radiation and solar materials to direct conversion of solar energy into electrical energy. In addition, readers will find important articles exploring other renewable energy sources. This journal places a strong emphasis on applications such as solar devices for home and industrial uses, solar heating and cooling systems, solar power systems and units, and agricultural uses of solar energy.

Journal of Solar Energy Science & Research

Journal of Solar Energy Science & Research

(Volume No. 8, Issue No. 1, January - April 2024)

Contents

Building integrated Performance of Single Slope and Multiple Effect Solar Still

Mohd Zaheen Khan, I. Nawaz,
Department of Mechanical Engineering
Faculty of Engineering & Technology
Jamia Millia Islamia New Delhi-110025
Email : zhnkhan4@gmail.com

ABSTRACT

In future we will not only consume energy, we will also partly produce our own energy need. Solar energy has been proven to be a valid strategy for producing on-site renewable energy. Planning for integrating solar energy in buildings involves many players and decision-making. In this article, a process map defining which decisions regarding solar energy needs to be discussed in which design stage, is presented. With the help of this process map, more informed decisions should facilitate the implementation of solar energy in buildings. Our way of thinking about energy and buildings is changing; initially buildings were solely considered to be energy-consuming, future buildings will be need to consume less energy while producing part of their own energy [1]. One way to produce renewable energy on-site is by means of active solar energy. By doing so, buildings will reduce the impact on the environment and reduce the dependence on imported energy. Current legislation is already directing towards such energy efficient and energy producing buildings, with the European directive for the energy performance of buildings [2] as the clearest example.

Keywords: Solar energy, Solar Still, Solar Desalination, Building integrated Desalination

1.0 INTRODUCTION

There are a number of processes that can be used to convert brackish water or saline water to fresh water. These include reverse osmosis, electro dialysis and distillation. Distillation is one of the simplest and widely used processes. More than 90% of the world's water desalination processes use distillation.

In the distillation process water is evaporated, leaving behind the impurities and microbiological organisms, thus vapour contains only fresh water molecules. The vapour should be condensed to get the fresh drinking water. The energy required for distillation can be provided by electrical energy or thermal energy. Since the vaporization of the water requires low temperature (around 100^0c), solar radiation energy can easily be used to achieve such low temperatures. The use of solar thermal energy

for distillation is similar to the rain cycle of the earth. Solar radiation falling on earth causes evaporation of water, forming clouds, which then get condensed in the cooler regions and bring backwater to the surface. In this way, solar distillation is effective in removing many unwanted impurities as listed below.

Salts and minerals: Na, Ca, As, Fl, Fe, Mn, etc.

Bacteria: E. coli, cholera, etc.

Parasites: Giardia, Cryptosporidium, etc.

Heavy metals: Pb, Cd, Hg, etc.

Solar water distillation technology has a long history. Installations were built over 200 years ago, although to produce salt water rather than drinking water. Documented use of solar stills began in the sixteenth century. An early large scale solar still was built in 1872 to supply a mining community in Chile with drinking water.

Mass production occurred for the first time during the Second World War when 2,00,000 inflatable plastic were made to be kept in life crafts for the US Navy. India is blessed with plenty of sunshine. Most of the country gets about 300 sunny days, resulting in daily solar radiation of about 4-7 kWh/m2. Therefore, solar distillation technology can be implemented effectively. Design and implementation of solar distillation apparatus is easy and cost effective. In the application of solar energy, like conversion of brackish or saline water into fresh water, intermittent supply of solar radiation should not limit its use, as the fresh water is produced as and when solar radiation is available.

2.0 OPERATION OF SOLAR DISTILLATION

A solar still apparatus is built on the same principle as rainwater cycle consisting of two steps, evaporation and condensation. In this way, the basic principles of solar water distillation is simple yet effective. The sun's energy heats water to the point of evaporation. As the water evaporates, water vapour rises, condensing on the glass surface for collection. This process removes impurities such as salts and heavy metals as well as eliminates microbiological organisms. In the end, water is cleaner than the purest rainwater. A schematic diagram of solar distill is shown in the Figure 1 on the next page.

A single basin solar still has a top cover made of glass. It has an interior surface made of a waterproof membrane. This interior surface uses a blackened material to improve absorption of the sunrays. The glass has a property to be transparent tovisible light but opaque to ultraviolet and infrared light. Therefore, the glass cover of a solar still allows visible part of solar radiation to pass into the still, which

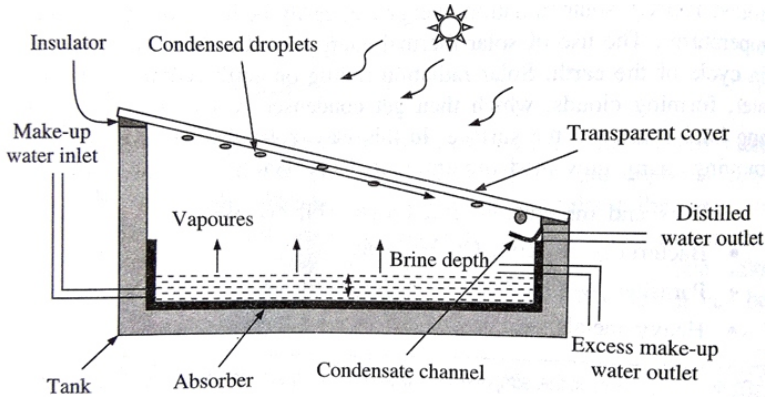

Figure1: Schematic layout of Single Slope Solar Still

is mostly absorbed by the blackened base, resulting in increase in basin temperature. Low temperature object radiates in the infrared region. Due to this, the basin radiates energy in the infrared region, which is reflected back into the still by the glass cover, thus, trapping the solar energy inside the still (glass cover absorbs infrared radiation and reradiates part of it back to the basin).

This is similar to a greenhouse effect. Due to this, the water heats up by about 10-20^{0}C, resulting in increased rate of evaporation. The moisture content of the air trapped between the water surface and the glass cover increases. The heated water vapour evaporates from the basin and condenses on inside of the glass cover in the form of small droplets. The condensation at glass cover occurs due to lower ambient temperature outside the glass cover.

These drops of water flow into condensate collection channels on the sides, which can be collected externally. In this process, the salts and microbes that were in the original water are left behind. Condensed water trickles down the inclined glass cover to an interior collection through and out to a storage bottle. The long axis of the solar still should be placed along the East-West direction such that the glass sloping is facing towards the south.

3.0 COMPONENTS AND SPECIFICATIONS

Various components of solar still and their specifications are summarized in Table 1.3 Refer to the still schematic given in above section.

System components	Specifications	
	Material	Purpose
Water basin/ Tank	Cement concrete or fiberglass	Container of saline water
Insulation	Polyurethane Foam, putty, tars	To prevent heat losses
Transparent cover	Glass or polyethylene	To transmit solar energy

Absorber	Black Butyl rubber, black polyethylene or ink or dye	To absorb the heat
Condensate channel	Aluminium, galvanized iron	To collect droplets of water
Make up water inlet	PVC pipe	To supply the saline water
Excess make-up water outlet	PVC pipe	To drain the water
Storage pot	Glass, Plastic	To store distilled water

4.0 SOLAR STILL DESIGN AND COSTING

4.1 Energy requirement and efficiency

The energy required to evaporate water is the latent heat of vaporization of water. The Latent Heat is the heat that is required by a substance to change its phase, from solid to liquid or liquid to gas or vice versa. The latent heat of evaporation of water is about 2260 kilojoules per kilogram. This implies that in order to produce 1 litre of water through distillation, heat input of 2260 KJ is required. In practice, one has to supply much higher amount of heat energy because the efficiency of the still will not be 100%.

Heat could be lost due to conduction, convection and radiation. There are several possible heat loss paths in solar still, such as heat could be lost due to vapour leakage, heat loss at the bottom and sidewalls of the still through conduction, heat loss due to radiation, heat loss due to convection from the glass cover, heat absorbed by the cover, etc. The overall heat loss could be 40 to 60%. Based on this information, the efficiency of solar still could vary in the range of 30% to 45%.

4.2 Design of the solar still

Design of the solar still is very simple. One aim of the calculation is to find out how much distilled water we will get per day from one square metre area and how much total area is required to fulfill our requirement. Following assumptions can be taken into account:

1. Latent heat of water evaporation – 2260 kJ/kg
2. Density of water – 1 kg per litre
3. Efficiency of Solar still – 0.30
4. Average daily solar radiation on a given location – 6 kWh/m2- day
5. Amount of distilled water required per day – 15 litres

Step 1: Useful solar radiation

Daily available solar radiation = 6 kWh/m^2-day

Useful solar radiation = Daily solar radiation x solar still efficiency

= 6 x 0.3 = 1.8 kWh/m^2- day

Step 2: Litres of distilled water produced per day per square metre

Latent heat of water evaporation = 2260 kJ/kg

Number of litres of distilled water produced per square metre per day efficiency of the system

$$= \frac{Useful\ solar\ radiation}{Latent\ heat\ of\ water\ evaporation}$$

$$= \frac{6480}{2260}$$

= 2.86 litres/m^2-day

Step 3: Total area of the solar still to fulfill the requirement

Total distilled water requirement per day = 15 litres/day

Total area of the solar still to fulfill family requirement

$$= \frac{Total\ daily\ Requirement}{Number\ of\ litres\ produced\ per\ day\ per\ square\ metre}$$

$$= \frac{15}{2.86}$$

= 5.23 m^2

Alternatively the total solar distill area required to fulfill daily requirement can be calculated using following formula

$$A = \frac{Q\ X\ 2.26}{G\ X\ E}$$

Where,

A- Total distill area required

Q- Total distilled water required per day

G- Daily solar radiation in MJ/m^2- day

E- Efficiency of solar distill in decimal

4.3 Economics of Solar Still

Payback period can be calculated using the calculation for distilled water used in battery maintenance. According to the calculations shown in section 1.11 a solar distill with 30% efficiency will produce about 2.86 litres per day per square metre if the daily solar radiation is 6 kWh/m^2-day.

Calculation of payback period for solar distill unit

Daily-distilled water production per unit area

= 2.86 litre/day

Cost of manufacturing of solar distill for one square metre area

= Rs 1500/m2

Cost of distilled water in the market

= Rs 10/litre

Worth of distilled water produced everyday

= 2.86 x 10 = Rs. 28.6/day

The number of days required to recover the cost of solar distill

$$= \frac{Cost\ of\ manufacturing}{Cost\ gain\ per\ day}$$

$$= \frac{1500}{28.6} = 52.31 = 53 \text{ days}$$

Thus, it can be seen that the payback period for solar distill is within 2 to 3 months.

4.4 Maintenance and troubleshooting

Some precautions must be taken for the good performance of solar still. They are as follows:

1. Cleaning the basin and flushing: As water evaporates from the solar still basin, salts and other contaminants are left behind. Over time, these salts can build to the point of saturation if the still is not properly maintained and flushed on a regular basis. Properly operating a still requires about three times as much make up water as the distillate produced each day. If the still produced 2 litres of water, then 6 litres of make up water should be added. The additional 4 litres water leaves the still as excess make up water. The excess make up water flushes the still basin through the overflow to prevent salt buildup.

2. Cleaning the glass and condensate channel: The glass cover must be cleaned periodically to remove the dust from the cover, which otherwise absorbs some part of the solar radiation reducing the efficiency of the solar distill. Care must be taken to avoid the breakage of glass, which may lead to vapour leak. Condensate channel also must be cleaned periodically while draining out the basin water. Glass can be cleaned with distillate itself or any other available cleaning solution.

4.5 Multiple Effect Solar Still

To improve this low efficiency, multiple effect solar still (MES) have been studied in many groups[6-8]. In MES, water evaporates on the first wick condenses on the condensation surface of second plate,

which has second evaporating wick on its opposite side. Therefore, the latent heat of condensation can be reused to evaporate the water in the second wick. (Fig. 1) By staking multiple layers of the condensation-evaporation plate, the heat of condensation can be reused multiple times to increase its efficiency. By stacking 11 layers, Tanaka et al. [6] obtained more than 10 litter per m^2 per day under sunlight about 20MJ/(m^2day), which is comparable to higher than 3.5 tons per year.

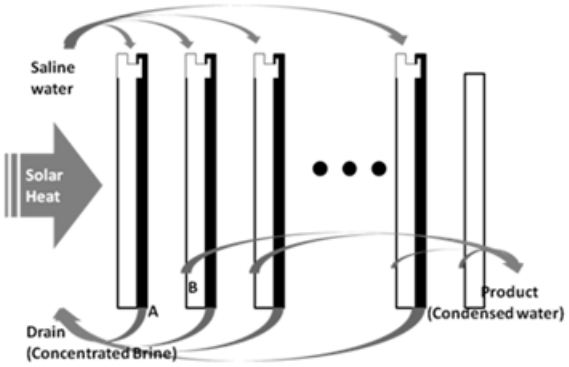

Figure: 2 Concept of multiple effect solar still: Saline water dripping through wick(A, Black) evaporates and condenses on the condensing plate (B, White), while concentrated brine drains to waste. The latent heat emitted during the condensation process heat the next wick for evaporation.

The system cost may include not only the Multi Effect Still itself, but also the installation cost which includes land, labour and structure material. This installation cost, especially the land cost, is almost linearly proportional to the size of the system. Therefore, if we install many Multi Effect Stills in separate bare land, substantial amount of budget would be required.

We can overcome this problem, by installing Multi Effect Still as part of building component. Since Multi Effect Still has panel shape, which can be positioned vertically or diagonally, it can be placed on the wall or rooftop. This is similar concept to Building Integrated Photovoltaicin solar power generation. Similar to photovoltaic panels in Building Integrated Photovoltaic, Multi Effect Still panels may replace concrete or tiles of outdoor structure of buildings, walls or fence facing sunny direction of the location.

Cost of land and installation may not make big matter in this "Building Integrated Desalination", since such cost is already required for making the same structure even without Building Integrated Desalination. Only the additional cost is required to add water supply and drain line to the structure, which might be partially compensated by the saved cost of the building material.

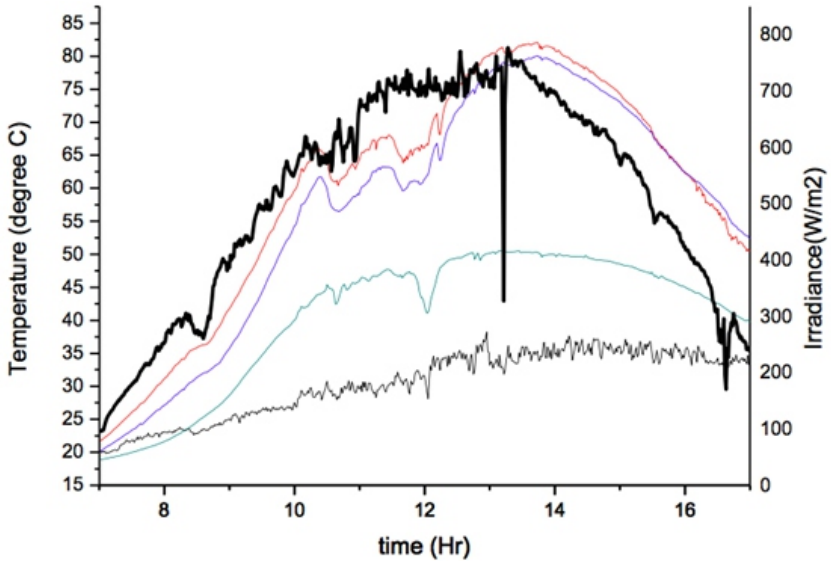

Figure: 3 Irradiance and temperature inside of black insulating plate

Figure 3 represents the solar irradiation and the temperatures with the system measured at New Delhi, on May 29th, 2016. Since each layer is cooled by evaporating water, it takes some time to heat up the layers by solar heat. Therefore, there is some right shift of the layer surface temperature graph from the solar irradiance graph. Adding proper amount of water is very important to operate the system efficiently. Deficient feeding may cause drought of evaporation wick, lowering the efficiency and failure of the system. Too much feeding may cause loss of heat so that large portion of water drained out even before evaporation occurs. Tanaka et al. [6,8] suggested around 1.6~2 for optimum feeding rate to evaporation rate ratio. In other words, the ratio of drain to the condensate should be in the range of 0.6~1. For proper water feeding, automatic flow controller was initially planned for the MES system. However, unfortunately, it was not ready at the time of measurement. Therefore, water was supplied under manual control, which was not very successful. Total solar energy on the active area during the period was calculated to be 1.38MJ by integrating the irradiation curve (6.31MJ/m2) multiplied by the active area (0.219m2). During the period, the MES system produced 283g of fresh water. Therefore, performance of 205g/MJ was calculated. In other word, under condition of 20MJ/m2/day, the system may produce about 4.1 litters per square meter daily. This is less than half of the expected value (more than 10 litter per square meter daily) described in above introduction. However, considering that this is a preliminary test, and we used MES with only 6 layers on current measurement instead of 10, there would be some room for further improvement.

5.0 CONCLUSION AND FUTURE WORK

Concept and advantages of Building Integrated Desalination (BIDS) was proposed. It can be a practical

solution to supply fresh water to isolated societies that cannot afford huge costs of Mass-Desalination Plant. Low cost multiple effect solar still could be a plausible way to realize BIDS. Some primitive test was done for the Multi Effect Still system. Further improvement on performance and cost down would be developed and tested soon. Since each water deficient country has its own specific environmental condition as well as specific social and economic requirements of water desalination, collaboration with researchers in such countries would be helpful to speed up the development Actual field test with improved prototypes in such countries should be done in future.

6.0 REFERENCES

[1] NoreddineGhaffour, Thomas M. Missimer, Gary L. Amy. Technical review and evaluation of the economics of water desalination: Current and future challenges for better water supply sustainability. Desalination 2013; 309: 197-207

[2] NikolayVoutchkov. Desalination cost assesment and management: Water treatment academy; 2011

[3] Y.AL Khoshi, W.Mamhair, M.Alodan. Opportunities for solar thermal desalination in Saudi Arabia; 2012; http://solarthermalworld.org/sites/gstec/files/saudi_arabia_solar_thermal_desalination.pdf

[4] Soteris A. Kalogirou. Seawater desalination using renewable energy sources. Progress in energy and combustion science 2005; 31: 242-281

[5] http://solargis.info

[6] H.Tanaka, T. Nosoko, T.Nagata. Experimental study of basin-type, multiple-effect, diffusion-coupled solar still. Desalination 2002; 150: 131- 144

[7] Hiroshi Tanaka, YasuhitoNakatake, Katsuhiro Watanabe. Parametric study on a vertical multiple-effect diffusion-type solar still coupled with a heat-pipe solar collector. Desalination 2004;171:243-255

[8] Hiroshi Tanaka, YasuhitoNakatake. Factors influencing the productivity of a multiple-effect diffusion-type solar still coupled with a flat plate reflector Desalination 2005;186:299-310

[9] http://www.kredc.net

Mohd Zaheen Khan is the Research Scholar in the Department of Mechanical Engineering he is also the Guest Teacher in the Mechanical Engineering Department. He is taken the classes of B.Tech & M.Tech and also provide guidance to the students in their project work.
Email: zhnkhan4@gmail.com

Islam Nawaz is a Associate Professor in Department of Mechanical Engineering, Jamia Millia Islamia, New Delhi, India. He is engaged in teaching and research activities. Islam Nawaz has published several papers in various national and International Journals/Conferences and guided several M.Tech Projects in Thermal areas.. He is life member of deferent technical societies
Email: islamnwz@yahoo.co.in

Study of Solar Photovoltaic (SPV) Powered Thermal Comfort System

Salman Tamseel[1] ,Shah Alam[2], S.M.Mahmood[3]
[1]Al- Falah University,Dhauj, Faridabad, Haryana,
[2,3]Associate Prof. Mechanical Engineering JamiaMilliaIslamia, New Delhi

A B S T R A C T

Solar energy is one of the most available forms of energy on the Earth's surface, besides; it is very promising and generous. It is freely available to all nations as kind of renewable energy; solar energy is paid more and more attention in the world. Generally the comfort is obtained using fossil fuels, which are damaging our environment. Solar air conditioning system helps to minimize fossil fuel energy use.Air conditioning is essential for maintaining thermal comfort in indoor environments, particularly for hot and humid climates. In this project a specified space having size 10.25 x 6.02 x 3 m located at Hamdard Nagar, New Delhi, at latitude 28.58° N, 77.24° E longitude and the height above sea level is 216m is selected to maintain thermal comfort. The comfort temperature inside the room is maintained 25° Cwith relative humidity 60% against maximum outside temperature 43° C. First the heat load calculation has been done to determine the required cooling effect. It is found that 5TR capacity air-conditioner is required to provide comfort cooling. Next solar radiation on SPV has been computed to insure either sufficient input radiation is available to run 5TR air-conditioner. To determine the availability of solar energy on SPV Hay, Davies, Klucher and Reindl (HDKR) models is used. On the basis of analysis, it is found that 13.5 MJ/m^2 solar energy is available at SPV which is sufficient to run 5TR air-conditioner. On the basis of this available energy no of PV panels are calculated. The maximum watt power rating of one panel is taken as 1000Wp. This capacity panel is manufactures byElecssol. It is found that 18 panel are required to fulfill the cooling requirements. For the backup of power the batteries are selected and numbers of required batteries are calculated. By considering battery capacity 200Ah, number of day's autonomy two and DOD 60%, we need 3 batteries to ensure the supply during night.

Keywords: SPV modules, Empirical models, global solar radiation, tilted surface radiation, heat load, package air-conditioner, Thermal Comfort.

1.0 INTRODUCTION:

The energy which we use is supplied by burning fossil fuels. These fuels are finite, causing pollution and depleting in nature. Therefore there are efforts to use infinite sources such as solar radiation. Solar radiation data are a fundamental input for solar energy application such as photovoltaic, solar-thermal systems and passive solar design. The data should be reliable and readily available for design, optimization and performance evaluation of solar technology for any particular location. Due to lack of

measured data, it is necessary to estimate the solar radiation using available empirical models based on meteorological data. The solar radiation can play vital role to provide cooling during summer seasons. It is cost wise more effective method as compare to conventional methods of cooling.

Many studies have been done in the field of thermal comfort using solar energy as input. Zhai et.al. [1] had designed solar powered absorption system and optimize the performance of system between two absorption chillers. Balghouthi et.al [2] had studied the feasibility of solar powered absorption system in Tunisia. Mittal et.al [3] had studied solar absorption system in both heating and cooling in building. Al-Alili et.al [4] had used hybrid collector to run hybrid air-conditioner. The comparison of vapour compressor system with hybrid system had been also done. Chua et.al [5] had described the energy efficient cooling technology, innovative system designs and intelligent air control strategies in their research paper. Ronghui et.al [6] had evaluated the feasibility and applicability of liquid desiccant air-conditioning system. The study consist of a liquid desiccant ventilation system for dehumidification and an air handling unit for cooling. A part from solar thermal applications in the fluid of cooling, direct application of solar radiation using PV panels had been also discussed by many researchers. Li and Wang [7] have designed PV panels to run vapour compression refrigeration and cooling systems. They concluded that grid connected PV air-conditioning system is more economical. Farivar et.al [8] had analysis that solar irradiance is not monotonic during flight, when PV cells are located on the wings of solar powered aircraft. Daut et.al [9] had focused their study in design and construction of direct current air conditioning system integrated with PV system, consisting of PV panels, charge, inverter and batteries. Nikhil et.al [10] had proposed hybrid AC/DC solar powered home grid model based on load characteristic of home appliances working on a 220V, 50Hz system. The main drawback of solar energy systems are lack of accurate measured data. It is always not possible to measure data energy where because of costly measuring devices and long measuring duration. Therefore various models have been developed to determine the solar energy on tilted PV panel surface. In the present study HDKR model [11] has been used to determine solar radiation on tilted panels. In this we have tried to establish relation between cooling effect and solar radiation input at PV panel. The study shows that sufficient amount of solar energy is available to run air-conditioning, excluding various panel losses.

Nomenclatures:

H_o: Monthly Average daily extraterrestrial solar radiation (kWh/m^2-day)

I_{SC},G_{SC}: Solar constant 1.367 kW/m^2

N: Day of the year

H_g : Monthly average daily global solar radiation (kWh/m^2-day)

a, b: Angstrom constants (for Delhi a = 0.25, b = 0.57)

H_d: Monthly average daily defused radiation (kWh/m^2-day)

H_T : Total incident solar radiation on tilted surface (kWh/m^2-day)

$H_{T,b}$: Beam radiation on tilted surface (kWh/m^2-day)

$H_{T,d}$: Defused radiation on tilted surface (kWh/m^2-day)

$H_{T,r}$: Ground reflected radiation on tilted surface (kWh/m^2-day)

H_b: Monthly average daily beam radiation on horizontal surface (kWh/m^2-day)

R_b: View factor for beam radiation

R_r : View factor for ground reflected radiation

HDKR: Hay and Davies, Klucher Model

IMD: Indian Metrological Department

$F_{c\text{-}s}$: View factor for circumsolar diffused radiation

F_c-h_z: View factor for horizon brightening solar diffused radiation

E_{WO} Energy generated without loss

E_{gp} Energy generated after considering losses

E_{oc}Energy output of Converter

E_G Energy fed to the grid

Greek symbols:

γ : Azimuth angle (degree)

β: Tilted angle (degree)

ω: Hour angle (degree)

ω_s: Sunset hour angle for mean day of month (degree)

Φ: Latitude angle (degree)

θ: Angle of incidence (degree)

θ_z: Zenith angle (degree)

ε: Elevation angle (degree)

2.0 SOLAR RADIATIONS MODELS:

The following models are used to compute solar radiation on tilted SPV.

2.1 Liu and Jordan model [12]

In this model, the solar radiation on tilted surface is consider to be composed of three parts such as; beam, reflected from ground and diffuse fraction. It was assumed that the diffuse radiation is isotropic only; whereas, circumsolar and horizon brightening were taken as zero.Hence, $I_{T,D}= I_d[(1+\cos\beta)/2)]$, and the overall formula for computing the total radiation on tilted surface is proposed as sum of beam, earth reflected and isotropic diffuse radiation. Thus, $I_T$is given as follows.

$$I_T = I_b R_b + I_{\rho g}\left(\frac{1-cos\beta}{2}\right) + I_d\left(\frac{1+cos\beta}{2}\right)$$

2.2 HDKR Model (2006)

If the beam reflected and all terms of diffuse radiation such as isotropic, circumsolar and horizon brightening are added to the solar radiation equation, a new correlation develops called HDKR model [11]. It is basically the combination of Hay, Davies, Klucher and Reindl models. The solar energy irradiation on tilted surface is then determined as:

$$H_t = (H_b + H_d.A)R_b + H_{\rho g}\left[\frac{(1-cos\beta)}{2}\right] + H_d\left[(1-A)\frac{(1+cos\beta)}{2}\right]\left[1+sin^3\left(\frac{\beta}{2}\right)\right]$$

The HDKR model is selected for the purpose of study.

3.0 METHODOLOGICAL DATA:

For the purpose of analysis the measured meteorological data, for New Delhi (28.58° N, 77.20° E, 216 amsl) viz., global, diffuse and beam radiation on horizontal surface have been taken from Indian Meteorological Department (IMD), Pune that has been completed by Mani [13]

4.0 METHODOLOGY:

For this analysis we have selected a conference hall located, (28.58° N, 77.24° E) ground floor of a multi-storage building in Hamdard Nagar, New Delhi-110062. These conference rooms North, South and East wall are exposed to Sun and the West wall are surrounded by adjacent room. The conference room is design for 30 persons to sit at a time, there are twenty LED bulbs, six fans and one 3-D LED TV.

The adopted methodology is as follows:

4.1 Heat Load Calculation

Table 1.0

	SOURCES	LOAD (Watts)
	Heat gain from walls, roof, floor, door &	2871.136
	Solar heat gain through glass	302.4
	Heat gain from 30 person	2250
	Heat gain due to ventilation	3304.8
	Heat gain due to 3D LED TV	40
Sensible Heat	Heat gain due to lighting	60
	Heat gain due to fans	240

	Heat gain due to fresh air	1440
	TOTAL SENSIBLE HEAT GAIN	1.065×10508.336 = **11.2 kW**
	Heat gain from 30 person	1650
	Heat gain due to ventilation	1350
Latent Heat	Heat gain due to fresh air	588
	TOTAL LATENT HEAT GAIN	1.06x3588 = **3.8 kW**
TOTAL HEAT GAIN	**11.2+3.8 = 15 kW**	

Considering Factor of safety 15%, the Grand Total Heat load becomes 5TR**.**

4.2 Determination of Daily irradiation on tilted surface:

HDKR model is used to determine solar radiation on tilted surface. Table 1.1 indicates the available, global, beam, diffuse and extraterrestrial radiation on horizontal surface.

Table No: 1.1:Global, Beam, Diffuse and Extraterrestrial solar radiation at Horizontal Surface ($J/m^2/day$)

Months	**H_g (J/m^2)**	**H_d(J/m^2)**	**H_b(J/m^2)**	**H_o(J/m^2)**
April	1772000	380700	13942800	37066211
May	18068400	6512400	12733200	40039177
June	15930000	8060400	8564400	41026266
July	13161600	7326000	6379200	40404150
August	12682800	6573600	6890400	38041363
September	14576400	5310000	11930400	33789549

Table 1.2: Solar Radiation on Tilted Surface.

Months	n	δ	ω_s	H_t (J/m^2)		
				$\beta=\phi$	$\beta=(\phi-15^\circ)$	$\beta=(\phi+15^\circ)$
April	105	9.414	95.18	14373352.26	23712506.61	4187875.893
May	135	18.79	100.68	17115115.74	18661054.81	14758936.69
June	162	23.08	103.42	14428467.23	15890212.96	12426848.18
July	198	21.18	102.18	12233052.22	13246740	10798071.94
August	228	13.45	97.48	12801685.74	134100380.6	11689796.17
September	258	2.21	91.20	18663672.07	18368627.54	17966582.74

4.3 Estimate of Energy:

Table No: 1.3: Energy Consumption in a day

System DC (load)	Total Load (kW)	No. of hours in operation per day (11:30-16:30) hr	Energy consumed per day (kWh)
Air-Conditioner	17	5 hr	17×5 =85

4.4 Sizing and choice of components.

4.4.1Converter

DC to DC converter = 95%

$$\text{Converter Input Power} = \frac{17000}{0.95} = 17894.73 = 17.89473kVA$$

$$\text{Converter Input Energy} = \frac{85}{0.95} = 89.47 \text{ kWh} = 89473.68\mathbf{Wh}$$

High voltage are preferable because high voltage DC means less current and less current means less losses in power means thickness of wire decrease, ultimately cost will reduce.

4.4.2Batteries

Estimate of ampere-hour (E) = 89473.68Wh

System Voltage = 480 V =383.77 Ah

No of days autonomy (N) = 2

Depth of discharge (DOD) = 60%= 0.6

$$\text{Total Ah capacity of battery} = \frac{\text{E} \times \text{No of days of autonomy (N)}}{\text{DOD} \times \text{System Voltage}}$$

$$= \frac{89473.68 \times 2}{0.60 \times 480}$$

$$= 621.345 \text{ Ah}$$

Consider One battery Capacity = 200Ah

$$\text{No. of batteries} = \frac{621.345}{200} = \mathbf{3\ batteries}$$

4.4.3Daily Sunshine Hour (5 hours/day).

$$\text{Required power of PV modules} = \frac{89473.68}{5} = \mathbf{17894.73\ W\ or\ Wp}$$

Now, total 17894.73 Watt peak of PV modules will be required to supply the required energy. PV module rating is 1000 Wp.

$$\text{No of PV panels} = \frac{17894.73}{1000} = \mathbf{18\ panels}$$

4.4 PV array Loss:

Table No: 1.4: Energy fed to grid during April to September

At β= ϕ=28.58°

Months	$E_{WO}(J/m^2)$	$E_{gp}(J/m^2)$	$E_{oc}(J/m^2)$	$E_G(J/m^2)$
April	19486390.5	15374762.1	15067266.86	14991930.53
May	17115115.74	13272772.96	13007316.81	12942280.23
June	14428467.23	11319132.54	11092749.89	11037286.14
July	12088759.54	9646830.113	9453893.511	9406624.043
August	12801685.74	10273352.81	10067889.75	10017546.32
September	17934513.2	14392446.84	14104597.91	14034074.92

At $\beta = (\phi - 15) = 13.58^\circ$

Months	$E_{WO}(J/m^2)$	$E_{gp}(J/m^2)$	$E_{oc}(J/m^2)$	$E_G(J/m^2)$
April	30281794.12	23892335.56	23414488.85	23297416.41
May	18661054.81	14471648.01	14182215.05	14111303.97
June	15890212.96	12465872.07	12216554.63	12155471.85
July	13246760.12	10570898.52	10359480.55	10307683.15
August	13410380.6	10761830.43	10546593.82	10493860.85
September	17657997.84	14170543.27	13887132.4	13817696.74

At $\beta = (\phi + 15) = 43.58^\circ$

Months	E_{WO} (J/m^2)	$E_{gp}(J/m^2)$	$E_{oc}(J/m^2)$	$E_G(J/m^2)$
April	7669449.549	6051195.694	5930171.78	5900520.921
May	14758936.69	11445555.4	11216644.3	11160561.07
June	12426848.18	9748862.397	95553885.149	9506115.724
July	10798071.94	8616861.408	8444524.18	8402301.559
August	11689796.17	9381061.426	9193440.198	9147472.997
September	17273934.65	13862332.56	13585085.91	13517160.48

Table No: 1.5 Average Solar radiations falling on SPV without loss (W.O.L) and with loss (W.O) during summer season.

Months	Average (H_T) at $\beta=28.58^\circ$ (MJ/m^2)		Average (H_T) at $\beta=13.58^\circ$ (MJ/m^2)		Average (H_T) at $\beta=43.58^\circ$ (MJ/m^2)	
	W.O.L	W.L	W.O.L	W.L	W.O.L	W.L
April	19.48	15.37	30.28	23.89	7.66	6.05

May	17.11	13.27	18.66	14.47	14.75	11.44
June	14.42	11.31	15.89	12.46	12.42	9.748
July	12.08	9.6	13.24	10.57	10.79	8.61
Aug	12.80	10.27	13.41	10.76	11.68	9.38
Sep	17.93	14.39	17.65	14.17	17.27	13.86
Total	81.02/6	74.21/6	109.13/6	86.32/6	74.57/6	59.088/6
Total Avg	**13.5**	**12.368**	**18.18**	**14.38**	**12.42**	**9.848**

RESULT AND DISCUSSION

First heat load calculation has been done for a specified cooling space. It is found that total sensible heat and latent heat is 11.2 kW and 3.8 kW. The total heat load is 15 kW which are shown in Table 1.0. It is found that total required cooling load is equivalent to 5 TR. The maximum design outside temperature is taken as 43°C during summer and the comfort temperature inside the room is taken 25°C with relative humidity of 60%. Solar radiation on SPV has been calculated to insure either sufficient solar energy is available or not to run the 5TR Air-Conditioning. For the calculation of solar radiation on PV panel we have selected HDKR (Hay and Davies, Klucher and Reindl) model [11] to determine the solar radiation on tilted PV panel. The tilt angle β is taken as β=ϕ, β= ϕ-15, β= ϕ+15. β= tilted angle= 28.58° (NEW DELHI). The ground albedo is considered as 0.2 the extraterrestrial radiation is given in Table 1.1. Table 1.2 shows the daily solar radiation at β= ϕ= 28.58°, β= (ϕ-15) = 13.58° (summer), β= (ϕ+15) = 43.58° (winter) in different month of year at tilted surface by HDKR model. The availability of solar radiation during summer season is 13.5MJ/m^2 at β= ϕ, 18.18MJ/m^2 β= (ϕ-15) and 12.42MJ/m^2 β= (ϕ+15) as indicate in Table 1.2. This indicates that available energy is sufficient to run 5TR capacity window package type air-conditioner. Energy consumption by air-conditioner is given in Table 1.3. The PV arrays are subjected to various losses such as module temperature loss, loss due to dust, mismatch, cable loss and solar radiation loss etc. To analysis all the losses we found that it is about 23%. The total solar radiation falling on PV panel is given Table 1.4, for different months of year at β=ϕ=, β= (ϕ-15), β=(ϕ+15) with and without losses. The Table shows that at β=ϕ every fit to the grid. Excluding these losses availability total energy at SPV is 12.368MJ/m^2 at β= ϕ= 28.58°, 14.38MJ/m^2 β= (ϕ-15) = 13.58° and 9.848 MJ/m^2 β= (ϕ+15) = 43.58°as shown in Table No: 1.5. On the basis of this available energy we calculate no of PV panels. It is found that 18 panel are required to fulfill the cooling requirements. The maximum watt power rating of one panel is taken as 1000Wp. This capacity panel is manufactures byElecssol. For the backup of power the batteries are selected and numbers of required batteries are

calculated. By considering battery capacity 200Ah, number of day's autonomy two and DOD 60%, we need 3 batteries to ensure the supply during night.

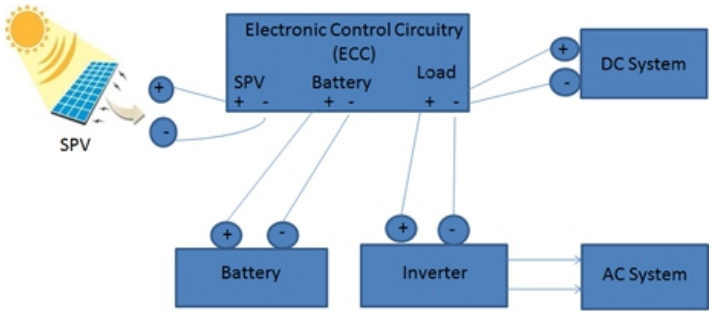

Fig.1.0 Final Actual System Cycle

CONCLUSION

This work focuses on either available solar radiation is sufficient to run air-conditioner. The design, construction and testing to run a high capacity package type system air-conditioner using solar energy integrated with photovoltaic (PV) system has been done in this study. In this work we have calculated solar radiation on PV Panel by using HDKR model (2006). The availability of solar radiation during summer season is 13.5 MJ/m^2. This energy subjected to various losses, these losses are analyzed and found that it is about 23%. Excluding these losses availability total energy at SPV is 12.368 MJ/m^2. This indicates that available energy is sufficient to run 5TR capacity window package type air-conditioner. On the basis of this available energy we need 18 PV modules of 1000Wp. To fulfill the requirement of input energy during night to air-conditioner, we need 3 batteries 200Ah with DOD 60%.

References:

[1]X.Q.Zhai, R.Z.Wang, J.Y.Wu, Y.J.Dai, Q.Ma. Design and performance of a solar powered air-conditioning system in a green building. Applied Energy, 2008; 297-311

[2] M.Balghouthi, M.H.Chahbani, A.Guizani. Feasibility of solar absorption air-conditioning in Tunisia. Building and Environment, 2008; 1459-1470

[3] V.Mittal, K.S.Ksan, N.S.Thakur. the study of solar absorption air-conditioning systems. Journl of Energy in Southern Africa, 2005, Vol16,4,59

[4] A.Al-Alili, Y.Hwang, R.Radermacher, I.Kubo. A high efficiency solar air-conditioning using concentrating photovoltaic/ thermal collectors. Applied Energy, 2012; 93, 138-147

[5] K.J.Chua, S.K.Chou, W.M.Yang. Achieving better energy-efficiency air-conditioning – A review of technologies nd strategies. Applied Energy, 2013; 104, 87-104

[6] Ronghui Qi, Lin Lu, Yu Huang. Energy performance of solar-assisted liquid desiccant air-conditioning system for commercial building in main climate zones. Energy conversion and management, 2014; 88, 749-757

[7] Y.Li, R.Z.Wang. Photovoltaic-powered solar cooling systems. Advance in solar heating and cooling, 2016; 227-250

[8] FarivarFazelpour, MajidVafouipour, OmidRhbari, Reza shirMohammddi. Considerable parameters of using PV cells for solr-powered air craft. Renewble and Sustainble Energy Reviews, 2013; 27, 81-91

[9] Daut, M.Adzrie, M Irewanto, P.Ibrhim, M.Fitra. Solar Powered air-conditioning system. Internationlconfrencs-Advancements in Renewable Energy and Clean Environment, 2013, 444-453

[10] Nikhil Sasidharan, NimalMadhu M, Jai Govind Singh, WeerkornOngsakul. An approach for an efficient hybrid AC/DC Solar Powered Homegrid system based on the load Characteristic of home appliances Energy and Building, 2015; 108, 23-35

[11] J.Duffie and W.A.Beckman. "Solar Engineering of Thermal Processes".2006; 3rd Ed. John Wiley & Sons, Inc.USA.

[12] B.Y.H.Liu and R.C.Jordan, The Internationals ship and Characteristic distribution of direct, Diffuse and total solar radiation. Solar Energy, 1960; 14(3), 1-9

[13] Mani A. Handbook of Solar radiation data for India, 1981; Allied Publication Pvt.Ltd, New Delhi

Solar Robotic Systems: A Review

[1]Mr. Mohammad Waseem, [2]Ms. EramNeha, [3]Dr. Mohd. Suhaib
[1]Research Scholar
Department of Mechanical Engineering, JamiaMillia Islamia
New Delhi-110025, India.
waseem2k14@gmail.com
[2]Research Scholar
Department of Mechanical Engineering, JamiaMillia Islamia
New Delhi-110025, India.
eramneha@gmail.com
[3]Professor
Department of Mechanical Engineering, JamiaMillia Islamia
New Delhi-110025, India.
msuhaib@jmi.ac.in

ABSTRACT

In last two decades, Automation and artificial intelligent improves accuracy as well asquality of product andreduced processing time due to enormous advancement in the technology of robotics. At present time, the most crucial factors in modern world are scarcity of energy resources for global demand. Due to environment issues and legislative straining, electrification is a glaring inclination to renovate performance and sustainability of transportation system. Solar photovoltaic technology is an important research area to convert the solar energy into useful electrical power. Solar robot extracts electrical energy stored in the batteries to runs its mechanical, electrical and electronic devices to perform the several tasks for industrial as well as commercial work. Robot can operate in a hazardous environment for long duration of timewithout human assistant with a highaccuracy.
Index Terms: Solar Electric Vehicle (SEV), Hybrid Vehicle (HV), Autonomous Guided Vehicle (AGV), Mars Exploration Rovers (MER), Photovoltaic (PV)

I. INTRODUCTION

Energy crisis are the prime issue in the world at present time as fossils fuel and uranium are the only available conventional energy resources while uranium is mostly used for nuclear power production and its need greater attention. So the main sources of energy available are fossils fuels like petroleum, coal and natural gas. Combustion by-products of fossils fuels contain a number of harmful gasses as carbon dioxide and carbon monoxide etc. These gaseous by-products resultdamage of ozone layer in

earth atmosphere and increment in global warming [1]. Internal combustion engines technology is the most widely used technology in existing transportation system while the world population and energy consumption increases, vehicles emission are dominating environmental issues such as air, land and water pollution [2]. Renewable resources of energy such as biomass production, wind kinetic energy, geo-thermal energy and solar cells technology getting more attention due to their non-polluting nature, eco-friendly and environment safety meritorious characteristics [3].

The automobile industry is undergoing a revolution in designing new electrical platforms for vehicles so as to counter the sophistications involved with engine and carbon emission issues. Seeking Electric drives not only troubleshoots the pollution issue but introduction of more electric controls imparts accuracy and precision in the ways of power & vehicle handling. The automobile industries introduced hybrid electrical vehicle to minimize the application of combustion engine by integrating electric drive system i.e. electric motor. This technology has a positive environment effect and creating zero pollution [4]. Autonomous guided vehicles (AGVs) are the robots which employed intelligent system to transfer effectively material and goods from one pick up point to another drop-up destination in ware houses, manufacturing system, hospitals etc. In-fact AGVs areinnovative electrical vehicle producing zero emissions at tail point [5].

In case of solar robots, solar energy can be stored in batteries and electric drives are the best means of converting this stored energy in batteries into useful mechanical work to drive the vehicle. Robots utilizing solar energy photovoltaic technology are the most promising new advancement in robotics and automation. These robots are self-generative (i.e. do not require an external power source) and save a great deal of energy. But harnessing solar energy in robots has its own disadvantages. Solar power is very irregular and very large panels are required to create small quantities of power. In this paper, applications of solar robotics system are reviewed.

II. REVIEW OF AGV

Autonomous guided vehicles (AGVs) are an important issue in automotive industry due to their safety, comfortability and flexibility.Autonomous guided vehicle which have the ability to self-locate their position and find out the feasible path for motion execution on terrain, these vehicle are better referred as “self-moving vehicle” or “unmanned guided vehicle”. AGVs are getting more importance in industrial as well as in transportation system to enhance the accuracy and quality of manufacturing with better time supervision. AGVs play an important role for developing and under developing countries to speed up production and accuracy of product in hazardous industrial environment for human workers.

G. Villagra and D. H. Parez [6] has presented fuzzy and vector pursuit based non-linear control techniques for robust path tracking in industrial environment by automated guided vehicles during load transfer operation. S. Butdee and A. Suebsomran [7] and A. A. Nayak et al. [8] has discussed image processing vision based technique for automated guided vehicles moving from starting point to reach its destination while path is not clear or discontinuity in guide line.

Navigation system of an autonomous vehicle is primary aspect as it must be able to sense its position, navigate its way toward goal and avoid obstacles it encounters. Y. Abe et al. [9] has presented vision based navigation system with variable template matching for autonomous mobile robot to diagnose landmark of different size by optimizing evolution strategy methodology. C. Wang et al. [10] presented improved vision based navigation system with fuzzy control algorithm for automatically transport equipment i.e. AGV which has low cost, easy installation and electromagnetic interference. M. Wiβing et al. [11] submitted a hybrid navigation system for meacnum rooted omnidirectional automated guided vehicles having a classical guidance system for offline managing process and an online active system for clashes rectification in dynamic mode environment situation by employing open transportation control system. R. Cucchiara et al. [12] addressed stereo vision based navigation system to develop an integrated framework, obstacle detection, ability to impart self-location and efficient monitoring in real time for autonomous guided vehicle at indoor as well as outdoor working applications. A. V. Gulalkari et al. [13] presented a kinect camera sensor operated object tracking and following system for four wheel independent steering automated guided vehicle using kalman filter and stepping control technique to calculate the global position and velocity coordinates of moving object. S. Sahoo et al. [14], proportional and proportional integral (PI) controllers has been designed and implemented to get the desired heading angle during vehicle dynamics for an autonomous ground vehicle (AGV).. M. B. Duinkerken and Lodewijks [15] summarized research towards performance improvement of automatic transport system for free ranging and positioning capabilities of AGVs by creating promoted routing techniques. They designed and developed an embedded vehicular controller with a real time operating vision navigation system for a two wheel differential driven AGV to improve its working performance, cost and reliability.

III. REVIEW OF SEV

There is scarcity of natural resources to produce adequate electricity as compare to demand by the people and industry in Bangladesh, even no electricity supply for the rural areas. Secondly due to high population and large no. of conventional vehicle (auto rickshaw) utilizing fossils fuel, increasing pollution and traffic jam problems. Control and Application Research Group of BRAC University Dhaka, Bangladesh has implemented and evolved in two project namely solar battery charging station

and torque sensor based electricity assisted rickshaw to resolve these major energy crisis. Solar battery charging station implantation can help solar electrification process in rural region as well as sustain the extra load of grid in urbanized areas. The battery charged on the charging stations can be employed to power the efficient and environmental friendly transportation system (rickshaw) which maintains the advance need while changing the dependency on carbon emission fuels by T. Faraz and A. Azad [16]. N. Shaha and M. B. Uddin [17] proposed hybrid energy based electric auto rickshaw is proposed for the purpose to find out an efficient model vehicle having enhanced range of driving capacity, fast speed of vehicle, enhanced life- time and better travelling competency. Battery bank of electric auto rickshaw is charged in two ways first by plug-in charging method and secondly solar photovoltaic technology during operation mode of vehicle. Solar energy availibity in the different cities of Bangladesh throughout the year is surveyed to support the construction of electrical auto rickshaw prototype. Fixed, installation and maintenance cost of electric vehicle is estimated to compare the cost with conventional auto rickshaw. ADVISOR software was employed to examine the hybrid electric vehicle performance, fuel economy and efficiency.

A.M. Paudel and P. Kreutzmann [18] Globally, fossils fuel based transportation is the key transportation, causing unexpected outcomes such as air, noise pollution, changes in climate, deficiency in natural visibility, accidental issues and water as well ground sealing problems. These factors are responsible to contributing pollution for economical and atmospherically sustainability while one third of worldwide energy is consumed by United State in transportation, taking major part in CO2 emissions. A hybrid tricycle design for a sustainable need of local commute is presented as an alternative means to revamp these factors and reducing energy consumption. Z. Preitl et al. [19] solar hybrid vehicle (SHV) is an advancement form of hybrid vehicle mounted photovoltaic solar cells technology to utilized renewable energy as an alternate source of energy. A mathematical model has been developed for this HSV which consists of internal combustion engine, electric motor, solar panel, and management unit for vehicle to make power balance between powers of electric generator, power obtained from PV panels, battery nominal power and electric power. Nonlinear and quasi piecewise linear mathematical model for generator load torque, motor dynamics, generator behaviour and battery model derived by assuming bilinear term as linear parameter varying system. Controllability and stability of design control system condition were studied, analysed and simulation performed to optimized fuel consumption of HSV. S. Fang et al. (2015) (k1)[20] presented uninterrupted mechanical transmission (UMT) driveline control system for electrical vehicle to improving vehicle dynamics, economics and comfort performance of vehicle as government body emphasizing strict restriction on usage fossils fuel and their emissions due to increase in atmosphere pollution, global warming and scarcity of oil resources. To imparting consolidated shifting between the two gears, an epicyclic gearing

system, a centrifugal clutch and a brake band has been employed in the presented UMT. Fuzzy Logic Control (FLC) having optimal control strategy at decision module layer of the controller has been executed in the supervisory strategy of transmission system for targeting accurate shifting processes with gearing module system. T. Sarkar et al. [21] presented electrical power system design and development of a solar electrical vehicle which utilized the photovoltaic solar panel to extract solar energy and converts into useful electrical energy to drive the electrical system. In the presented approach, they employed Brushless DC motor for solar electrical vehicle due to better operating characteristics such high torque, high efficiency low inertia and need less space compared to DC motor.

IV. REVIEW OF SOLAR ROBOTS

Various robots which utilized the solar power to perform different tasks discussed are summarized as below:

Satellite solar power station (SSPS) concept to meet the future energy demand in space based on photovoltaic conversion technology is represented by P.E. Glaser [22]. Design and performance analysis of mars exploration rovers with solar array to accumulate the excessive dust during mission was presented by M. Stella et al. [23]. S. Lukic et al. [24] presented autonomous solar auto rickshaw having electrical actuator to propel the vehicle and batteries charged by renewable solar energy that operate in an eco-friendly way to replaced LPG and CNG based conventional auto rickshaw. T. Deor and Y.S. Angal [25] presented design and construction of an optimized charging system for Li-Po batteries with the aid of tracked solar panels for a VANTER robotic exploration vehicle. F.G. Cordova and A.G. Gonzalez [26] proposed an intelligent navigation system for unmanned under water vehicle powered by solar renewable energy to measure the physical and chemical parameters of water quality inspection on predefined paths for long distances. N. Riaz et al. [27] explained design and fabrication of automated personal mobility vehicle (wheel chair) with retractable solar panels to help handicaps.

V. CONCLUSION

Robots are intelligent machines in modern world with various synthesis of technology to alleviate the human endeavour and provide optimized output for the task assigned to them. Autonomous guided vehicles are the mobile robots that automatically transport desired equipment/part to enhance automation in logistic system. Electrical energy powered vehicles are getting more attention in place of conventional fuel based transportation system to solve environment issues such as pollution and global warming. One of the most reliable renewable energy resources is solar energy which is abundant in nature. In this paper, combing these two concepts various solar powered robots are discussed and reviewed.

REFERENCES

[1] B. Masood, R. A. Naqvi, and R. M. Asif. "Designing of A Control Scheme For The Solar Rickshaw In Comparative Study With Conventional Auto Rickshaw" 4th International Conference on Engineering Technology and Technopreneuship (ICE2T), pp. 324-329, 2014.

[2] M. Alahmad, M. A.Chaaban and L. Chaar, "A Novel Photovoltaic/Battery Structure for Solar Electrical Vehicles [PVBS for SEV]" IEEE Vehicle Power and Propulsion Conference, pp. 1-4, 2011.

[3] M. G. Simaes, N. N. Franceschettiand J. C. Adamowski, "Drive: System Control And Energy Management Of A Solar Powered Electric Vehicle" Applied Power Electronics Conference and Exposition (APEC). vol. 1, pp. 49 – 55, 1998.

[4] M. A. Hannan, F. A .Azidin and A.Mohamed, "Hybrid electric vehicles and their challenges: A review" Renewable and Sustainable Energy Reviews, vol. 29, pp. 135-150, 2014.

[5] S. G. M. Hossain and M. Y. Ali, "Automated Guided Vehicles for Industrial Logistics - Development Of Intelligent Prototypes Using Appropriate Technology" The 2nd International Conference on Computer and Automation Engineering (ICCAE) vol. 5, pp. 237-241, 2010.

[6] J. Villagra and D. Herrero-Perez. "A Comparison of Control Techniques For Robust Docking Maneuvers of An AGV" IEEE Transactions on Control Systems Technology, vol. 20, no..4, pp. 1116-1123, 2012.

[7] S. Butdee and A. Suebsomran. "Automatic Guided Vehicle Control By Vision System". IEEE International Conference on Industrial Engineering and Engineering Management, pp. 694-697, 2009.

[8] A. A. Nayak, et al. "Robotic Navigation In The Presence of Static and Dynamic Obstacles". Annual IEEE India Conference (INDICON), pp. 952-955, 2012.

[9] Y. Abe et al. "Vision Based Navigation System By Variable Template Matching For Autonomous Mobile Robot". Proceedings. IEEE International Conference on Robotics and Automation (Cat. No.98CH36146) vol. 2, pp. 952-957, 1998.

[10] C. Wang et al. "Development of A Vision Navigation System With Fuzzy Control Algorithm For Automated Guided Vehicle". IEEE International Conference on Information and Automation, pp. 2077-2082, 2015.

[11] M. Wißing et al. "Hybrid Navigation System for Mecanum Based Omnidirectional Automated Guided Vehicles". Proceedings of 41st International Symposium on Robotics ISR/Robotik pp. 1-6, 2014.

[12] R. Cucchiara, E. Perini, and G. Pistoni. "Efficient Stereo Vision For Obstacle Detection And AGV Navigation". 14th International Conference on Image Analysis and Processing (ICIAP 2007), pp. 291-296, 2007.

[13] A. V. Gulalkari et al. "Kinect Camera Sensor-Based Object Tracking And Following Of Four Wheel Independent Steering Automatic Guided Vehicle Using Kalman Filter". 15th International Conference on Control, Automation and Systems (ICCAS) pp. 1650-1655, 2015.

[14] S. Sahoo, S. C. Subramanian, and S. Srivastava. "Design And Implementation Of A Controller For Navigating An Autonomous Ground Vehicle". 2nd International Conference on Power, Control and Embedded Systems pp. 1-6, 2012.

[15] M. B. Duinkerken and G. Lodewijks. "Routing Of AgvsOn Automated Container Terminals". IEEE 19th International Conference on Computer Supported Cooperative Work in Design (CSCWD) (2015): pp. 401-406, 2015.

[16] T. Faraz and A. Azad. "Solar Battery Charging Station and Torque Sensor Based Electrically Assisted Tricycle"

Global Humanitarian Technology Conference, pp. 18-22, 2012.

[17] N. Shaha and M. B. Uddin. "Hybrid Energy Assisted Electric Auto Rickshaw Three-Wheeler" International Conference on Electrical Information and Communication Technology (EICT), pp1-6, 2013.

[18] A. M. Paudel, and P. Kreutzmann, "Design And Performance Analysis Of A Hybrid Solar Tricycle For A Sustainable Local Commute". Renewable and Sustainable Energy Reviews, vol.41, pp. 473-482, 2015.

[19] Z. Preitl, B. Kulcsar, and J. Bokor, "Piecewise Linear Parameter Varying Mathematical Model of A Hybrid Solar Vehicle" IEEE Intelligent Vehicles Symposium, pp. 895-900, 2008.

[20] S. Fang, et al. "Design And Control Of A Novel Two-Speed Uninterrupted Mechanical Transmission For Electric Vehicles". Mechanical Systems and Signal Processing 75 (2016):pp.473-493, 2016.

[21] T. Sarkar, M. Sharma, and S. K. Gawre. "A Generalized Approach To Design The Electrical Power System Of A Solar Electric Vehicle" IEEE Students' Conference on Electrical, Electronics and Computer Science, pp. 1-6, 2014.

[22] P.E. Glaser. "The Potential of Satellite Solar Power". Proceedings of the IEEE vol. 65, no. 8, pp. 1162-1176, 1977.

[23] P.M. Stella, R.C. Ewell, and J.J. Hoskin. "Design And Performance Of The MER (Mars Exploration Rovers) Solar Arrays". Conference Record of the Thirty-first IEEE Photovoltaic Specialists Conference, pp. 626-630, 2005.

[24] P. Mulhall et al. "Solar/Battery Electric Auto Rickshaw Three-Wheeler". IEEE Vehicle Power and Propulsion Conference (2009): pp. 153-159, 2009.

[25] T. Deore and Y. S. Angal. "Optimization of Battery Charging System in Solar-Powered Robotic Vehicle Using Microcontroller". ITSI Transactions on Electrical and Electronics Engineering (ITSI-TEEE): vol. 2, no. 3, pp. 2320 – 8945, 2014.

[26] F. G. Cordova, and A. Guerrero-Gonzalez. "Intelligent Navigation For A Solar Powered Unmanned Underwater Vehicle". International Journal of Advanced Robotic Systems. Vol. 10, 2013.

[27] N. Riaz and J. B. Aamir. "Electrical Wheel Chair With Retractable Solar Panels". International Conference on Energy Systems and Policies (ICESP) (2014): pp. 1-6, 2014.

Influence Of Local Winds On The Post-Monsoon Wave Characteristics In The Shallow Waters Off West Coast Of India

[1]DST-Woman Scientist, CSIR-National Institute of Oceanography, Goa, India 403 004
[2]Principal Scientist, CSIR-National Institute of Oceanography, Goa, India 403 004
Email: jkerkar@nio.org, jay@nio.org

ABSTRACT

Prediction of coastal waves using the state of the art wind wave models requires reliable input wind parameters. Global wind databases, such as NCEP/NCAR reanalysis winds, ERA-INTERIM winds, CFSR winds, etc., and mostly used in the wind-wave models as input, neither resolves the local winds nor the extreme winds during storms; also these wind data sets do not resolve the wind variations close to the coast. Therefore, the wind wave models often fail to capture the effect of local winds during normal conditions. Few studies exist on the influence of winds on waves in nearshore regions on the west coast of India, however these studies did not consider the measured local winds collocated with wave measurements. The influence of local winds, obtained from collocated measurements of winds and waves at two different locations on the west coast of India is studied in this paper. The contribution of local winds in generation of seas is studied through a state of the art numerical spectral wind wave model. The spectral wind wave model is forced with measured local winds, global wind induced waves along the boundaries and a combination of measured local winds and global wind induced waves along the boundaries. The model results were compared with measurements of seas and swells and the contribution of local winds on wind seas is evaluated from the model results.

Keywords: Spectral wind wave model; swells; seas; local winds; NCEP/NCAR reanalysis winds; ERA-Interim winds; NCEP-CFSR winds

1. INTRODUCTION

The knowledge of wave condition is vital for all marine related activities such as offshore and coastal structures. Wind blowing over the sea surface is the direct cause of surface wind wave generation and therefore, the quality of wind forcing used to drive a wave model is critical. Cavaleri et al. (1994) showed the direct dependency of significant wave height on wind speed through an empirical relationfor a fully developed sea. Sanil Kumar et al. (2000) studied that the wave height and wave

period predictions by a wave model is dependent on the precision of the wind field used as input. They also concluded that the error in the wave hindcast or forecast increases with decreasing frequency in wind speed. Feng et al. 2006 studied the impact of input wind forcing on the wave model. There are different sources of wind data with varying grid resolution, e.g., NCEP/NCAR reanalysis winds have a grid resolution of 2.5° (Kalnay et al,1996), ERA interim winds have a grid resolution of 0.125° (Dee et al. 2011), NCEP-CFSR winds have a grid resolution of 0.205° (Saha et al. 2006), etc. But these global winds do not provide reliable winds close to the coast and therefore the wind wave models using these winds fail to capture the effect of local winds. Earlier studies on waves in shallow waters along the Indian coast are mostly focused on (a) characteristics of measured waves (e.g., Aboobacker et. al., 2011, 2013; Dora and Sanil Kumar, 2015; Sanil Kumar et. al, 2014) and (b) numerical modelling of waves with various wind inputs and their comparison with measured or satellite derived waves (e.g., Vethamony et. al., 2006, 2011). Vethamony et al., (2006) used NCMRWF winds to simulate waves in the North Indian Ocean and the modelled wave parameters match reasonable match with measurements. Vethamony et al., 2011 pointed out that fine resolution winds are necessary to model the waves accurately, and understand the effect of land-sea breeze on wind-sea generation in the coastal regions. Glejin et al. (2013) studied the influence of winds (from ERA interim wind database) on waves in nearshore regions on the west coast of India through inverse wave age using land based coastal winds for wind seas and NCEP winds for swell systems. As the central theme of this study is to estimate the contribution of local winds on the coastal waves through wind wave modelling, wave model was forced separately with (a) local winds (b) global wind induced waves along the boundaries and (c) local winds combined with global wind induced waves along the boundaries. Thus far, to the knowledge of the authors, there haven't been any studies in the Indian coastal waters, related to waves and collocated measured winds. This work therefore would be a first to study and report the contribution and influence of measured local winds on the wind waves measured in coastal waters of India.

2. METHODOLOGY

Two locations on the central west coast of India, viz., off Mumbai and off Vengurla are considered in this study (Fig. 1), wherein collocated wave and wind data measurements at 10m water depth are available. These locations have similar offshore wave climate conditions and are subjected to similar climatic conditions with the southwest monsoon having dominant wave and wind climate compared to other periods. Post-monsoon wave measurements in coastal waters off Mumbai were measured using InterOcean® DWS4 directional wave and current measuring instrument, whereas, off Vengurla, a Datawell® directional wave rider buoy was used. Both these instruments provide time series of spectral wave parameters as well as time series of surface elevations from which the statistical wave parameters

can be derived. The main spectral wave parameter used in this study is the significant wave height (Hs). A weather station capable of measuring wind speed, wind direction, air temperature, humidity, etc was installed 10 m above sea on a vessel within 20 m radius of the wave measuring device. This measured wind speed and direction was considered uniform over the local region and was used to force the wave model to simulate local wind induced waves.

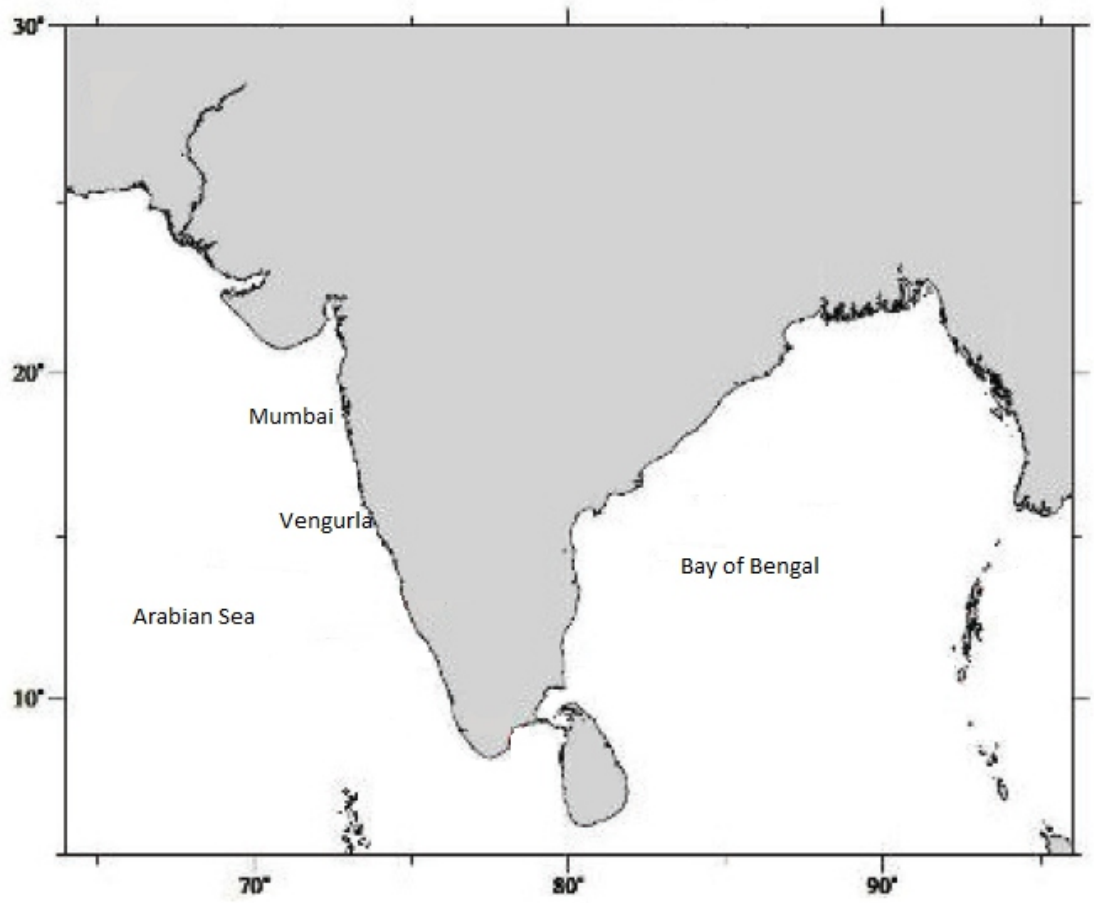

Figure 1 Location map

The measured waves contain both the swell and sea components. The sea component in the overall waves is due to the influence of local winds. The measured waves are analysed and the seas and swells components are separated through the 1-D separation method described by Portilla et al., (2009). The separation method algorithm calculates the ratio (γ) between the peak energy of a wave system and the energy of a PM spectrum at the same frequency. If γ is above a threshold value of 1, the system is considered to represent wind seas, else it is taken to be swell and a cut off frequency (fc) is estimated. Swell parameters are computed by integrating frequencies ranging from 0.025 Hz to fc and wind sea parameters are computed by integrating frequencies ranging from fc to 0.58 Hz. The separated sea and swell components as well as the overall wave heights are compared with the numerical wave model

forced with global wind data and local winds to ascertain by how much the inclusion of local winds would influence the numerical model results.

The MIKE by DHI spectral wind wave model (DHI, 2012), a state-of-the-art numerical tool for prediction of wave climate in offshore and coastal areas, was employed in this study. It includes a new third generation spectral wind-wave generation formulation model based on unstructured meshes. The MIKE-SW model includes two different formulations viz., Directional decoupled parametric formulation and fully spectral formulation, to simulate the growth, decay and transformation of wind-generated waves. In this study the fully spectral formulation has been used. The fully spectral formulation is based on the wave action conservation equation, where the directional-frequency wave action spectrum is the dependent variable. MIKE 21 SW includes the following major physical phenomena: (i) wave growth by action of wind, (ii) non-linear wave-wave interaction (iii) dissipation due to (a) white-capping (b) bottom friction (c) depth-induced wave breaking (iv) refraction & shoaling due to depth variations (v) wave-current interaction (vi) effect of time-varying water depth and flooding and drying. The discretization of the governing equation in geographical and spectral space is performed using cell-centered finite volume method similar to the hydrodynamic model. In the geographical domain, an unstructured mesh technique is used. The time integration is performed using a fractional step approach where a multi-sequence explicit method is applied for the propagation of wave action.

The input parameters used in wave model in the present study are the local winds measured off Mumbai and off Vengurla as well as three different sets of global winds. The global winds obtained are used to generate the long distant waves (swells) and the local winds are used to generate the local wind waves (seas). Three different global wind field data are used for the swell component; the first global wind field data used in the study is ERA-Interim winds available as 6-hourly mean zonal and meridional surface wind components, at a spatial square grid resolution of 0.125°. The second wind field used is the mean hourly CFSR winds from NCEP/NCAR with a spatial square grid resolution of 0.205°. And the third wind field data used is the NCEP/NCAR re-analysis wind data available as 6-hourly mean zonal and meridional surface wind components with a spatial square grid resolution of 2.5°. In order to obtain swell component and sea components from the wave model, three different input conditions were employed. Firstly, waves were simulated with global winds forced on a larger model domain comprising of the Indian Ocean and the waves obtained were considered as swell component of the over waves. These swells were extracted along the boundaries of the local domains (Fig. 2) and used to force the wave models for the local domain, thereby obtaining swell components in the local domain. Secondly, local winds measured collocated with wave measurements were used to force the local

domain models to obtain the sea component of the waves and thirdly both the local winds and swell components were forced along the boundaries, to obtain the overall simulated waves. Only the significant wave height derived from the wave model is used in this study.

Two local model domains as shown in Fig.2 are set up for two regions viz. off Mumbai and off Vengurla. A flexible mesh was generated using DHI tools and the bathymetry was taken from the NHO charts. The boundaries of these models are forced with the global wind data based induced waves extracted from a larger model domain comprising of the southern and northern Indian Ocean (not shown here due to lack of space), to obtain the swells. While these model domains are forced with the measured local winds to obtain seas. From the model results, significant wave heights are extracted at the measurement location and compared with the sea and swell components respectively for each of the model scenarios. The statistics of the comparisons are obtained and the influence of local winds on the overall waves is obtained in terms of the improvements in accuracy of the wave model predictions.

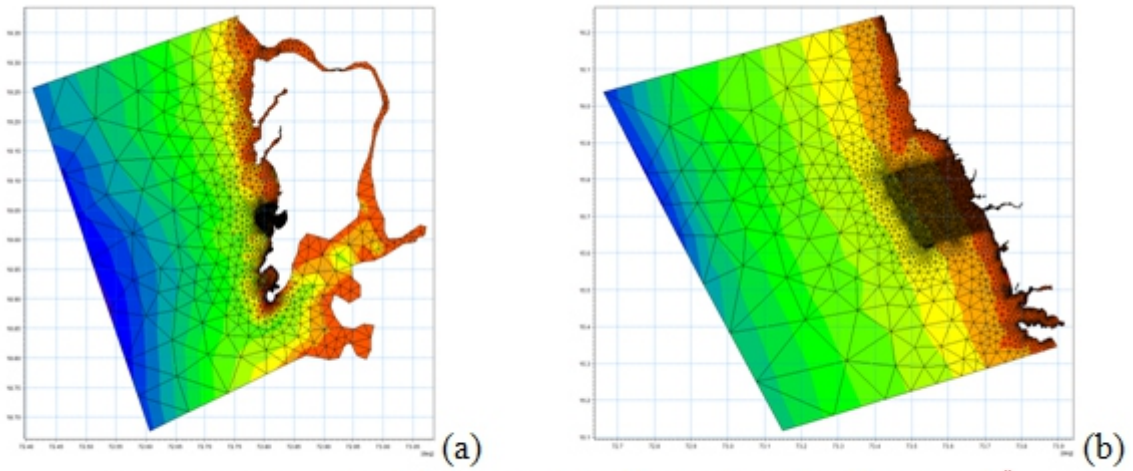

Figure 2 Wave model domain (a) off Mumbai (b) off Vengurla

Comment [JKS11]: India map, locations, model domain box, then this figure

3. RESULTS AND DISCUSSION

The measured waves off Mumbai and Vengurla along with the numerical model results for various scenarios are shown in Figs 3 to 6. The comparisons of measured significant waves (Hs) with the modeled Hs off Mumbai for ERA-interim, CFSR and NCEP wind data inputs with and without addition of local winds are shown in Fig. 3. The comparison of the sea component of the measured waves with the local wind induced waves is shown in Fig. 4. Similarly for Vengurla, comparison of measured significant waves (Hs) with the modeled Hs off Mumbai for ERA-interim, CFSR and NCEP wind data

inputs with and without addition of local winds are shown in Fig. 5 and the comparison of the sea component of the measured waves off Vengurla with the local wind induced waves is shown in Fig. 6. The statistical estimates of scatter index and correlation coefficient for Mumbai and Vengurla data are shown in Table 1.

It is observed that simulated waves obtained using CFSR or ERA-interim or NCEP wind in the Mumbai model domain do not capture the overall waves on their own. The ERA winds were observed to result in lower wave heights compared to CFSR or NCEP inputs for Mumbai case (Fig. 3a). Inclusion of local winds along with ERA slightly improved the resemblance of some of the measured wave features; however, these are not comparable with measurements. The CFSR wind induced waves were observed to provide the trend of the measured waves but not the variations observed in the measured wave heights (Fig. 3b). Inclusion of local wind along with the CFSR wind waves did not improve the simulated wave heights; moreover, inclusion of local winds along with the CFSR induced seems to have suppressed the swells. A better representation of the measured waves were observed from the NCEP wind induced waves wherein the wave height range is comparable to that of the measured wave heights (Fig. 3c). Inclusion of local winds onto the NCEP wind induced waves has shown considerable improvement in the overall wave generation for the Mumbai region. Comparison of measured sea wave component with the local wind induced waves (Fig. 4) for Mumbai region showed that not all the sea wave components are possible to be captured only from the local measured winds. However, majority of the sea wave components generated within the measurement region can be captured by including the collocated measured local winds off Mumbai.

Similar to the case as observed for Mumbai, the simulated waves off Vengurla obtained using CFSR or ERA-interim or NCEP wind in the model domain do not capture the overall waves on their own. All the three global wind induced waves were observed to result in lower wave heights for the period of simulation (Fig. 5). Even the inclusion of local winds along with the global wind induced waves did not improve the modeled wave features, except for the CFSR wind case (Fig. 5b). The local winds inclusion in the model produced increased waves at almost diurnal frequency that would be due to land-sea breeze prevalent in the region. Comparison of measured sea wave component with the modeled local wind induced waves (Fig. 6) for Vengurla region showed that majority of the sea wave components are possible to be captured by including the local measured winds. However, some of the sea wave components are still unable to be captured by including the collocated measured local winds off Vengurla.

Table 1 Scatter index and correlation of wave height comparisons for Mumbai and Vengurla

	Scatter Index		Correlation	
	Mumbai	Vengurla	Mumbai	Vengurla
ERA	0.6	0.6	0.15	0.35
ERA+LW	0.52	0.6	0.26	0.41
CFSR	0.43	0.43	0.18	0.19
CFSR+LW	0.81	0.41	0.25	0.28
NCEP	0.39	0.29	0.16	0.0023
NCEP+LW	0.35	0.84	0.27	0.12

[LW - local winds; ERA - ERA interim winds; NCEP - NCEP/NCAR reanalysis winds; CFSR - CFSR winds]

From the statistical analysis of the comparison between the measured and modeled waves, the scatter index and the correlation coefficients are considered here for discussion. For Mumbai data, the NCEP with local winds has shown the least scatter index whereas for Vengurla data, the NCEP data showed the least. Though the correlation between the measured and modeled waves is poor, the increase in correlation coefficient when the local winds are added is conspicuous in all cases.

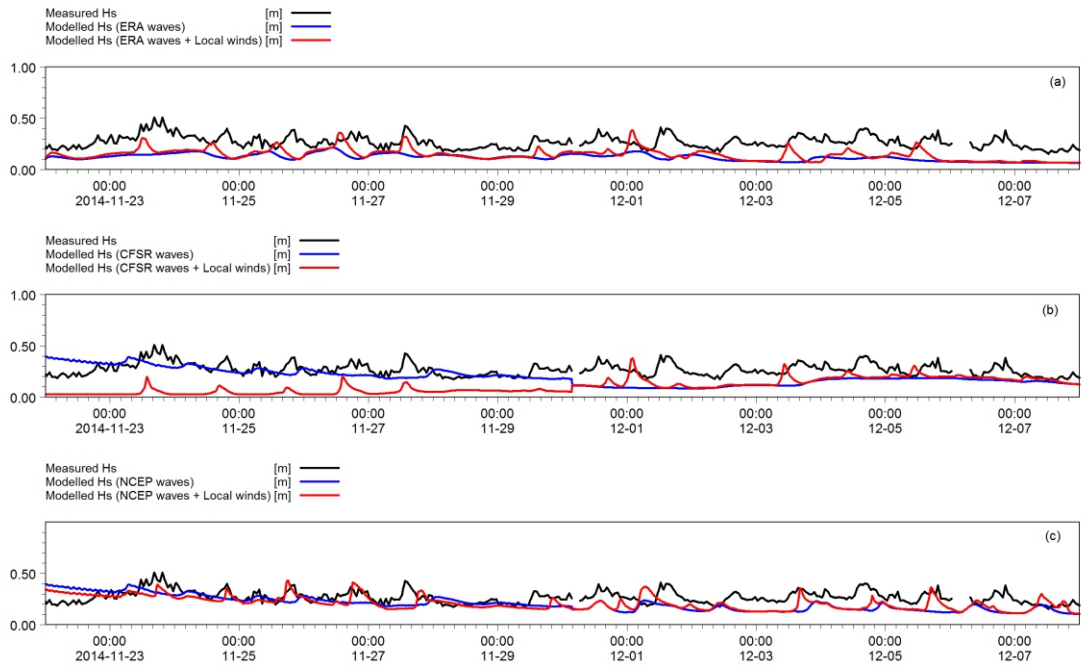

Figure 3 Comparison of measured Hs with modeled Hs off Mumbai (a) for ERA winds (b) for CFSR winds and (c) for NCEP winds

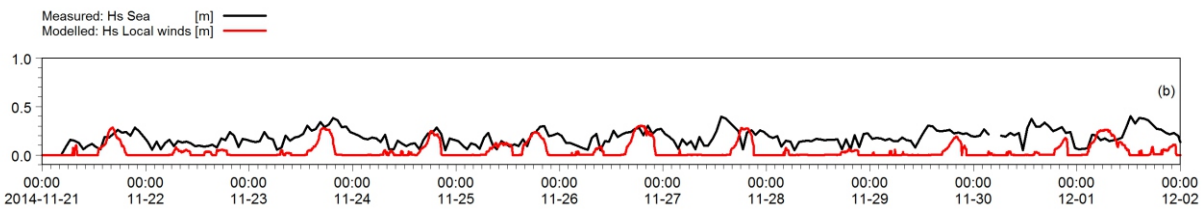

Figure 4 Comparison of measured seas Hs with modeled Hs with local winds

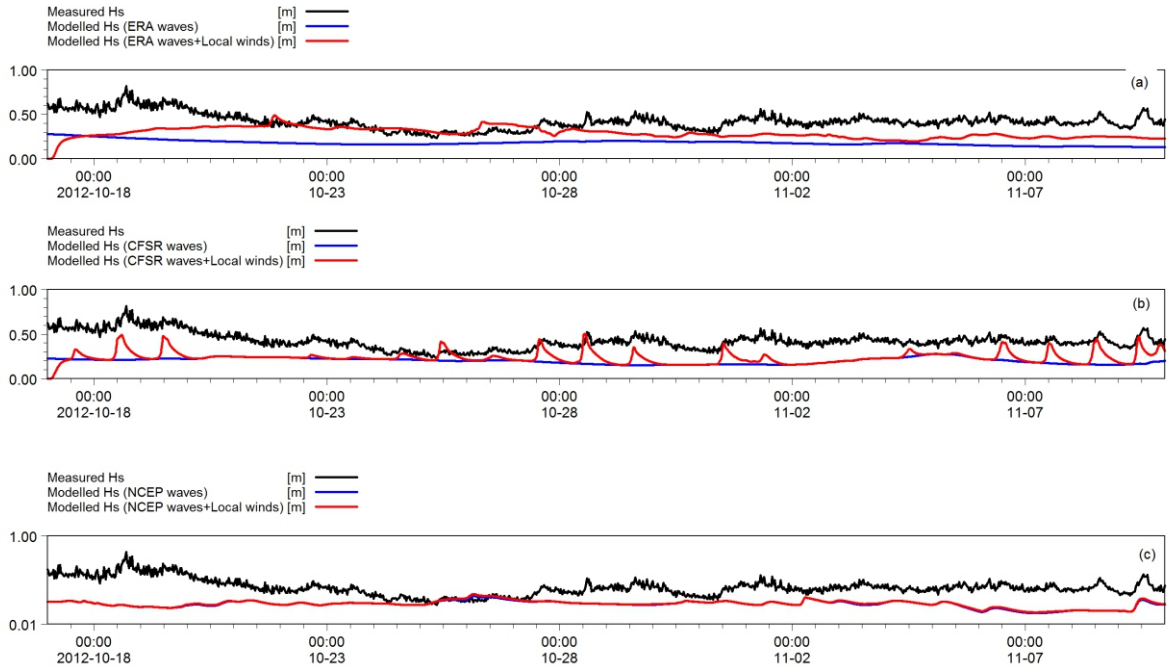

Figure 5 Comparison of measured Hs with modeled Hs off Vengurla (a) for ERA winds (b) for CFSR winds and (c) for NCEP winds

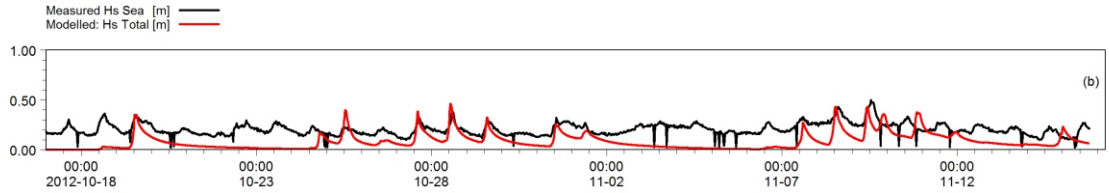

Figure 6 Comparison of measured seas Hs off Vengurla with modeled Hs with local winds

The influence of local winds on post-monsoon waves measured off Mumbai and Vengurla is the focus of this paper. This is carried out by establishing the significance of local winds in predicting the overall waves in the region utilizing three different global wind data sets used for wave prediction. Firstly, the analysis of measured waves showed that the seas generated by local winds were of the order of 0.1 to 0.4 m for Mumbai and 0.1 to 0.5m for Vengurla, whereas the overall wave heights were of the order of 0.2 to 0.8m for Vengurla and 0.2 to 0.5m for Mumbai. From the above information, it can be said that local wind induced waves are of significant magnitude during post-monsoon period.

The modeled Hs with different global wind induced waves clearly showed that on their own these global wind data sets are not sufficient to estimate the local wind induced waves in the nearshore waters. And it is also seen that inclusion of local winds along with the global wind input significantly improves the comparison with measured waves than the comparison with only global induced waves. Among the different sets of global winds induced waves CFSR winds along with local measured shows better comparison for Vengurla waves and the

than NCEP/NCAR winds combined with local winds provided better wave prediction for Mumbai region. It is also observed that the local measured winds (point observations) on their own are insufficient to completely decipher the local waves or seas, and therefore coastal wind observations over the region are essential to improve the predictability of overall waves including the seas.

4. CONCLUSIONS

The influence of local winds on the wave characteristics is studied through comparison of measured waves and waves obtained from numerical wave modeling in the nearshore regions of Mumbai and Vengurla. Three different global wind data sets viz., NCEP/NCAR reanalysis, CFSR and ERA-interim, were used to obtain the waves in the study regions and were found to underestimate the overall measured waves. It is observed that inclusion of winds measured collocated with wave measurements improve the wave modeling results, however, one point measurements of winds are found to be inadequate. Nevertheless, the importance of local winds is made clear by the improved correlation coefficient between modeled and measured waves. The local measured winds (point observations) on their own are insufficient to completely decipher the local waves or seas, and therefore coastal wind observations over the region are essential to improve the predictability of overall waves including the seas.

References

Aboobacker V.M, Vethamony P, Samiksha,S.V., Rashmi R., Jyoti, K., (2013), Wave transformation and attenuation along the west coast of India: measurements and numerical simulations Coastal Engineering Journal, Vol. 55(1),1350001 (21pages).

Aboobacker V.M, Rashmi R, Vethamony P, Menon HB, (2011). On the dominance of pre-existing swells over wind-sea along the west coast of India. Cont Shelf Res. 31:1701–1712

Cavaleri L 1994 Applications to wave hindcasting and forecasting; Chapter IV; In: Dynamics and Modeling of Ocean Waves, Cambridge University Press, UK, 532p.

Dee, D.P.1,, Uppala, S.M.1, Simmons, A.J.1, Berrisford, P.1, Poli, P.1, Kobayashi, S.2, Andrae, U.3, Balmaseda, M.A.1, Balsamo, G.1, Bauer, P.1, Bechtold, P.1, Beljaars, A.C.M.1, Van de Berg, L.4, Bidlot, J.1, Bormann, N.1, Delsol, C.1, Dragani, R.1, Fuentes, M.1, Geer, A.J.1, Haimberger, L.5, Healy, S.B.1, Hersbach, H.1, Hólm, E.V.1, Isaksen, L.1, Kållberg, P.3, Köhler, M.1, Matricardi, M.1, McNally, A.P.1, Monge-Sanz, B.M.6, Morcrette, J.J.1, Park, B.K.7, Peubey, C.1, De Rosnay, P.1, Tavolato, C.5, Thépaut, J.N.1 and Vitart, F.1*

DHI (2012). MIKE 21 Wave modelling - MIKE 21 SW - spectral waves FM short description, Horsholm, Denmark.

Dora, G., Sanil Kumar, V., (2015). Sea state observation in island-sheltered nearshore zone based on in situ intermediate-water wave measurements and NCEP/CFSR wind data, Ocean Dynamics, 65:647–663.

Feng H, Vandemark D, Quilfen Y, Chapron B and Beckley B 2006 Assessment of wind-forcing impact on a global wind-wave model using the topex altimeter; Ocean Eng. 33 1431–1461.

Glejin, J., Sanil Kumar, V., Balakrishnan Nair, T. M., Singh, J., (2013). Influence of winds on temporally varying short and long period gravity waves in the near shore regions of the eastern Arabian Sea, Ocean Science, 9, 343–353

Kalnay, E., Kanamitsu, M., Kistler, R., Collins, W., Deaven, D.,Gandin, L., Iredell, M., Saha, S., White, G., Woollen, J., Zhu, Y.,Chelliah, M., Ebisuzaki, W., Higgins, W., Janowiak, J., Mo, K., Ropelewski, C., Wang, J., Leetmaa, A., Reynolds, R., Jenne, R., and Joseph, D., (1996). The NCEP/NCAR reanalysis project, B. Am. Meteorol. Soc., 77, 437–471.

Portilla, J., Ocampo-Torres, F. J., and Monbaliu, J. (2009). Spectral Partitioning and Identification of Wind Sea and Swell. Journal of Atmospheric and Oceanic Technology, 107-122.

Saha, S., Nadiga, S., Thiaw, C., Wang, J., Wang, W., Zhang, Q., Van den Dool, H. M., Pan, H.-L., Moorthi, S., Behringer, D., Stokes, d., Peña, M., Lord, S., White, G., Ebisuzaki, W., Peng, P., and Xie, P., (2006). The NCEP climate forecast system. J. Climate, 19, 3483–3517.

Sanil Kumar, V., Ashok Kumar, K., Anand, N.M., 2000. Characteristics of waves off Goa, west coast of India. J. Coast. Res. 16 (3), 782–789.

Sanil Kumar, V., Shanas, P.R., Dubhashi, K. K., (2014). Shallow water wave spectral characteristics along the eastern Arabian Sea, Nat. Hazards, vol. 70(1), 377-394.

Vethamony P, Aboobacker VM, Menon HB, Kumar KA, Cavaleri L (2011). Superimposition of wind seas on pre-existing swells off Goa coast. J Mar Syst 87(1):47–54.

Vethamony, P., Sudheesh, K., Rupali S P., Babu, M.T., Jayakumar, S., Saran, A. K., Basu, Kumar, Kshatriya, (2006). Wave modelling for the north Indian Ocean using MSMR analysed winds, International Journal of Remote Sensing, 27(18), 3767-3780.

Spatio-Temporal Variation In Aerosol Optical Depth And Cloud Parameters Over India Retrieved From MODIS Satellite Data

[1]V. Lakshmana Rao, [2]P. Satish
[1]Assistant Professor,
Dept. of Meteorology & Oceanography,
Andhra University, Visakhapatnam, India
[2]Research scholar,
Dept. of Meteorology & Oceanography,
Andhra University, Visakhapatnam, India

ABSTRACT

Aerosols play an important role in cloud formation and subsequent precipitation. In the long run from climatological point of view, the gradually increase aerosol content leads to a change in earth atmosphere, heat balance and radiation balance leading to global warming and subsequent climate change. In the present study the spatial and temporal variations in aerosol particles over India were described. Here we are using moderate resolution imaging spectro radiometer (MODIS) data retrieved from the Terra satellite. High mean Aerosol Optical Depth (AOD) values are observed in almost in all regions during all the seasons. The spatial gradient of AOD shows an increase from southern part of Indian sub-continent to Northern part up to the Himalayas. The high AOD values are noticed during the winter and post monsoon seasons for the stations Delhi, Gandhi Nagar and Pune when compared to the other stations. This can be attributed the fact that they are urban, Industrial and coastal station. The correlation between AOD and Cloud fraction was found to be higher than that are coastal stations compared to continental. The correlation between AOD and CF was greater than 0.7 Gandhi Nagar, 0.5 in Visakhapatnam, 0.4 Jaipur and Pune and where as in Delhi, Anantapur, Ranchi and Trivandrum, it is (0.3, 0.3, 0.3 and 0.2) respectively. In this article we obseaverved that the AOD, Water vapor and cloud fraction shown negative correlation for all the five stations over the south India and observed positive correlation in North India for the remaining five stations.

Key Words: MODIS, aerosol optical depth, water vapor, cloud fraction and correlation coefficient.

I. INTRODUCTION

Atmospheric aerosols influence the earth's weather and climatic system in many ways, both directly and indirectly, although the magnitude of this influence remains uncertain even today(IPCC,2007).They have a direct effect through their ability to scatter and absorb solar radiation,

and an indirect effect through their fundamental role in cloud microphysics. They change the size and density of cloud droplets thereby modifying the cloud albedo, the cloud lifetime, and the precipitation(Twomey et al.,1984; Coakley et al; 1987; Kaufman and Fraser,1997;a,b; Ramanathan et al., 2001). Most publications to date show that increasing cloud condensation Nuclei (CCN) concentrations lead to higher cloud drop concentrations, to smaller effective radii and to longer-lived clouds (Albrecht, 1989; Ramanathan et al., 2001).

Furthermore, since smaller cloud droplets are less efficient in producing precipitation than larger ones, an enhanced aerosol population will lead to a longer cloud life (Rosenfeld, 1999, 2000). This phenomenon results in a lower rate of surface evaporation , a more stable and drier atmosphere, and consequently a reduction in cloud formation (Hansen et al., 1997).Clouds and water vapor play a changing role in radiative forcing, alternatively warming and cooling the earth. Heavy cloud covers during the shields the surface from incoming solar energy thereby cooling the earth.At night, clouds trap outgoing radiation thereby warming the Earth.

A great number of studies were conducted on the possible modification of cloud properties via the interaction with atmospheric aerosol particles, as this may lead to important changes of the Earth's climate. Biomass burning aerosols have been shown to affect clouds through both microphysical and radiative mechanisms (Kaufman and Koren, 2006; Koren et al.,2008; Rosenfeld et al., 2008). Biomass burning, from both deforestation and annual agricultural burning, is the largest anthropogenic source of such particles in the Southern Hemisphere; Biomass burning aerosols are hygroscopic and can serve as cloud condensation nuclei (Feingold et al; 2001; Andreae et al., 2004; Ten Hoeve et al., 2010). More recently, satellite analyses have revealed a persistent correlation between cloud fraction and aerosol optical depth in regions influenced by marine aerosol, smoke, dust and industrial air pollution (Loeb and Manalo-Smith, 2005; Kaufman et al., 2005).

This research focussed on two main objectives. The first was to investigate the seasonal, temporal and spatial variations of MODIS aerosol optical depth(AOD) over various major cities in southern India. The second objective was to analyze the relationships between AOD and various cloud parameters using correlation maps and time series plots, in order to understand the impact of aerosols (AOD) on cloud microphysics. The seasonal, spatial, and temporal variations in AOD and an investigation into the impacts of aerosols on cloud parameters are discussed in the present paper.

II. DATA AND METHODOLOGY

The MODIS sensor is on board of the polar orbiting NASA- EOS Terra and Aqua space crafts. Terra crosses the equator south ward about 10:30 local solar time (LST), where as Aqua north about 13:30(LST). MODIS views the earth in 36 channels from 0.41μm to 14 μm at a variety of spatial resolutions (250m, 500m and 1000m). Among the hundreds of products derived from MODIS-measured radiance is a suit of aerosols products (Levy et al.,2007) and another set of cloud products (king et al., 2003 and platnick et al.,2003), including aerosol optical depth (AOD), cloud top pressure and cloud fraction. Often the AOD is used as a proxy for the cloud condensation nucleus (CCN) concentration. The reliability of this proxy depends on the uniformity of the aerosol size, composition, vertical distribution, but may in many cases be used as a first approximation. AOD is provided as a 10km product and the cloud products are provided at 5x5, 1km resolution. To study the interaction between aerosol and clouds from satellite observations, information on both is needed, for the same time and location. However aerosol cannot be retrieved beneath clouds under cloudy condition by most satellite sensors, and cannot be retrieved above clouds by MODIS.

To solve such a problem the characteristic spatial scale of the aerosol field is assumed to be larger than that of a cloud so that it is sufficient to measure aerosols in the vicinity of the clouds. Often the retrieved resolution is decrease so the grid square size a much larger area compared to the retrieval resolution that leads to increase in the likelihood of information on clouds from the cloudy part and on aerosol from the cloud free part within the large grid square. The MODIS data are available at different processing levels, level 1.0(geolocated radiance and brightness temperature), level 2.0 (retrieved geophysical data products) and level 3.0 (gridded points) (king et al., 2003). MODIS uses infrared bands to determine the physical properties of cloud in relation to cloud top temperature and temperature, and visible and near infrared bands to determine optical and microphysical cloud properties (Jin and Shepherd, 2008; Remer et al., 2005; Levy et al., 2007).

For water vapor the retrieval for the near infrared is adopted. The selected 10 major cities in the study area are located in India (Fig:1) Thiruvananthapuram (8.85^{0}N,77.26^{0}E),Banglore(13.49^{0}N,77.95^{0}E), Anantapur (15.22^{0}N,78.42^{0}E), Pun e(19.39^{0}N, 75.16^{0}E), Visakhapatnam (18.53^{0}N,83.47^{0}E), Delhi (28.88N^0,77.33^{0}E), Ranchi (23.71^{0}N,85.89^{0}E), Jaipur (27.86^{0}N,76.28^{0}E), Kolkata (22.62^{0}N,88.40^{0}E), Gandhi Nagar (23.42^{0}N,73.03^{0}E) are the study areas shown in figure 1.

The above selected regions cover urban, coastal and rural environments. This study provides an opportunity to understand seasonal, temporal and spatial variations of MODIS aerosol optical depths

and cloud properties. We retrieved AOD and cloud parameter data for the period between 2004 to 2014 from the MODIS Terra satellite.

In the present study, we focused on the aod at wave length of 550nm over land, as this is close to the peak of the solar spectrum and is therefore associated with major radiative effects.

Study Area Map

Fig: 1 Geographical regions used in this mapSpatial Distribution of Annual means AOD, Cloud Fraction and Water vapor for the period 2004-2014

Fig: 2

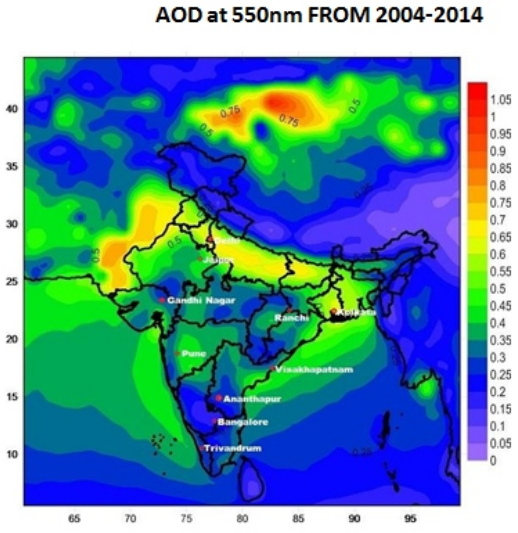

Fig: 3

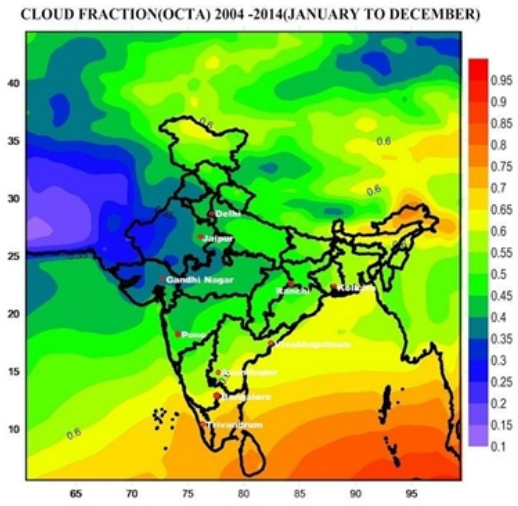

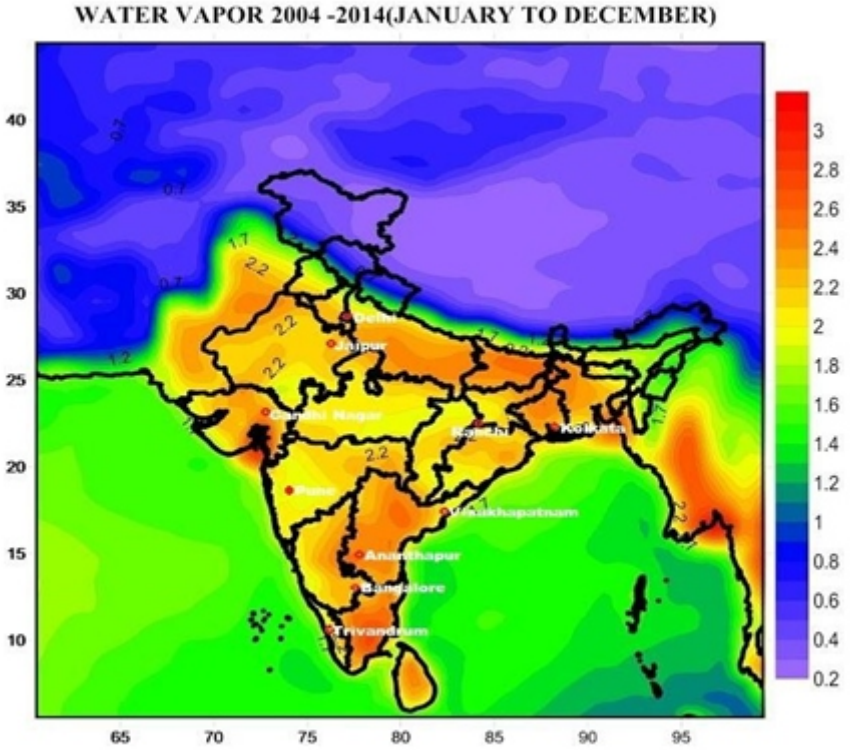

Seasonal studies of AOD for different seasons in India

Fig:5(a) **Fig:5(b)**

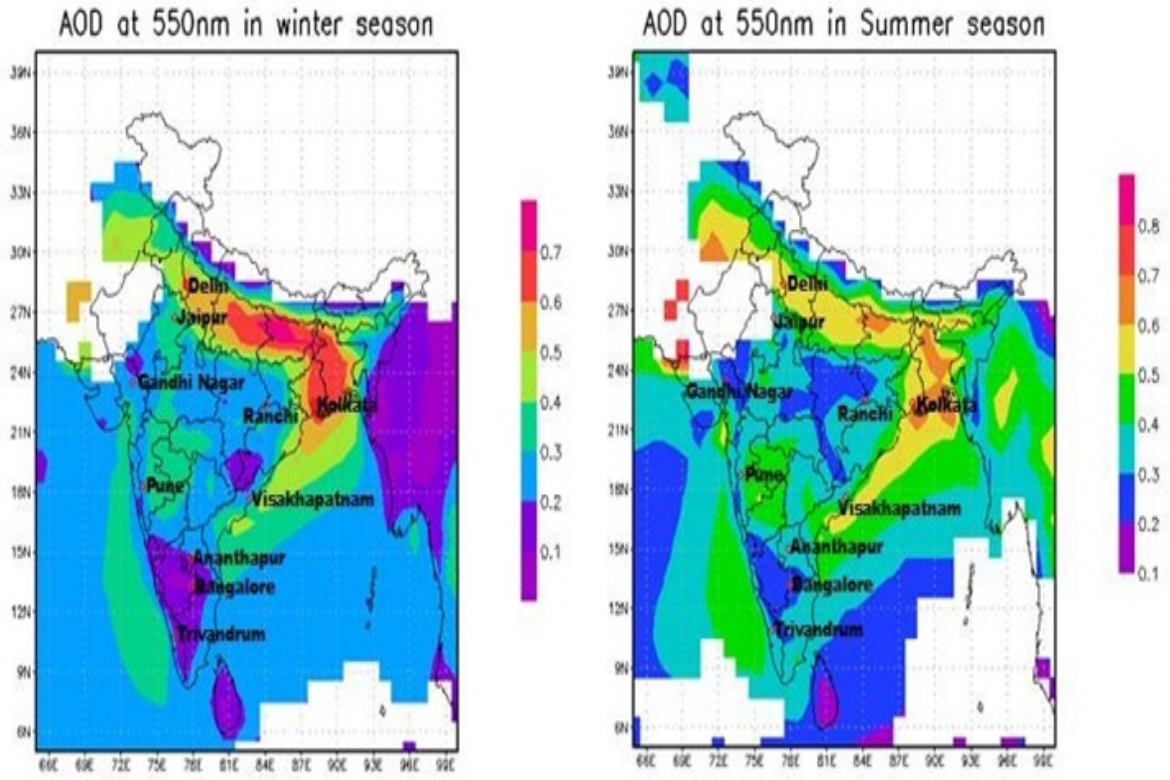

Fig:5(c)

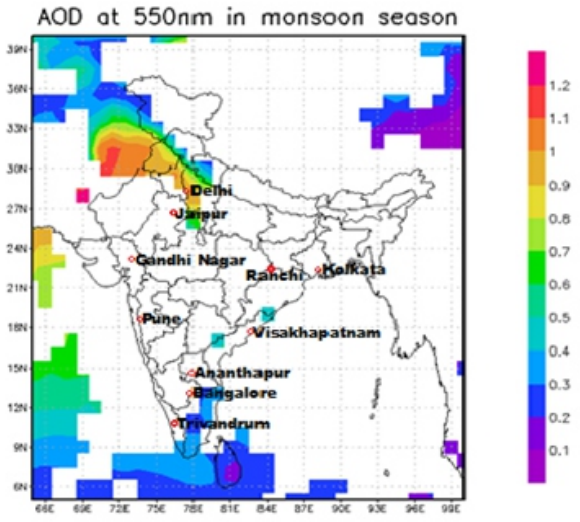

Fig:5(d)

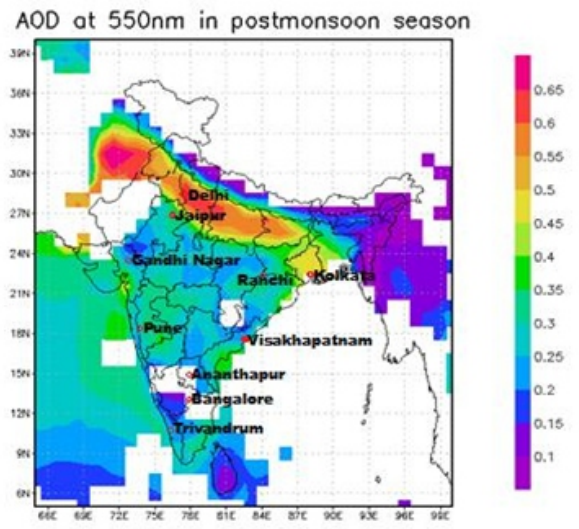

Spatial Correlation between AOD, Cloud fraction and Water vapor

Fig: 6 (a)

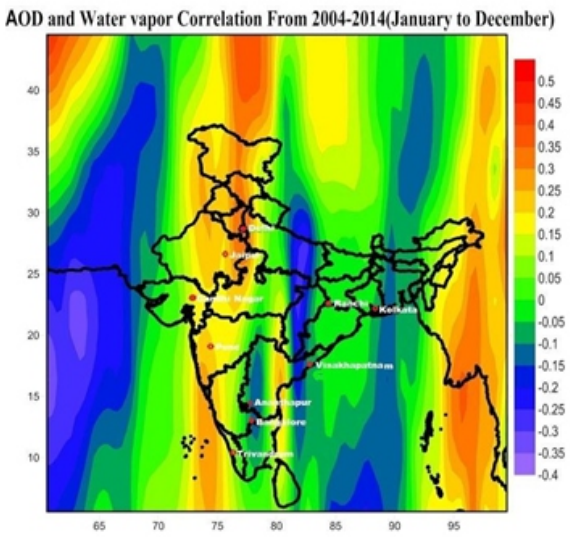

Fig: 6 (b)

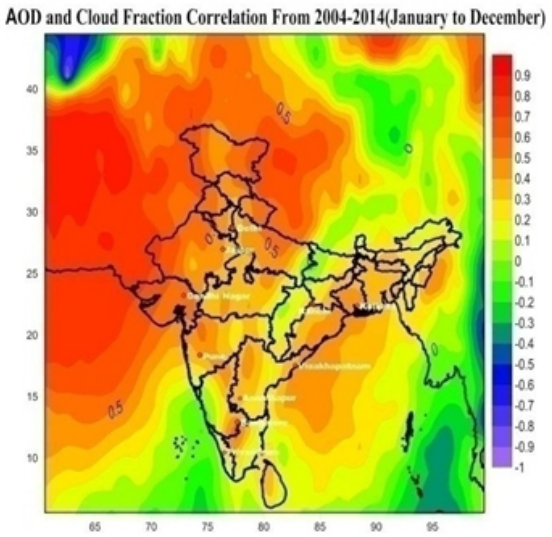

Fig:6 (c)

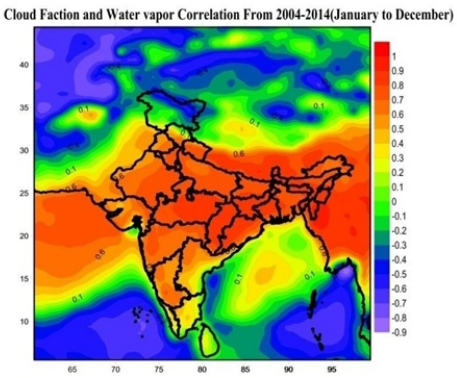

AOD VS WATER VAPOR **AOD VS CLOUD FRACTION**

Fig: 7(a) **Fig: 7(b)**

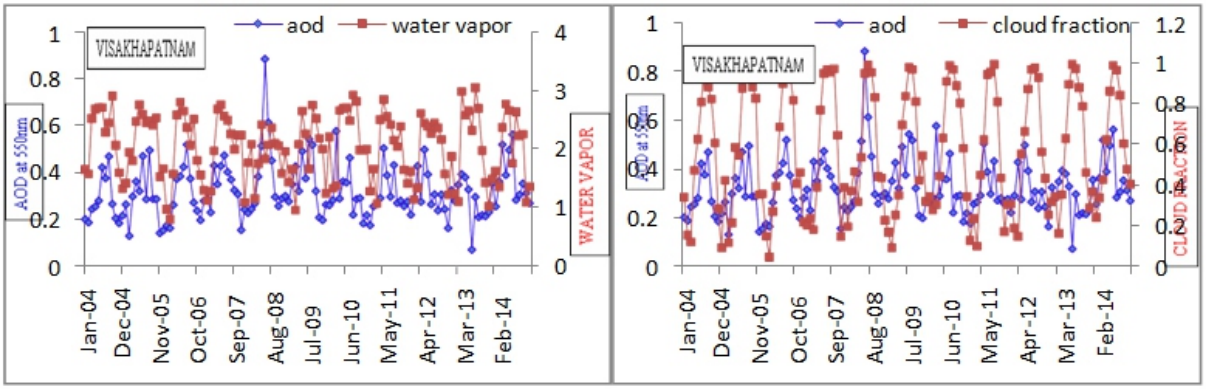

AOD VS WATER VAPOR **AOD VS CLOUD FRACTION**

Fig:7(c) **Fig: 7(d)**

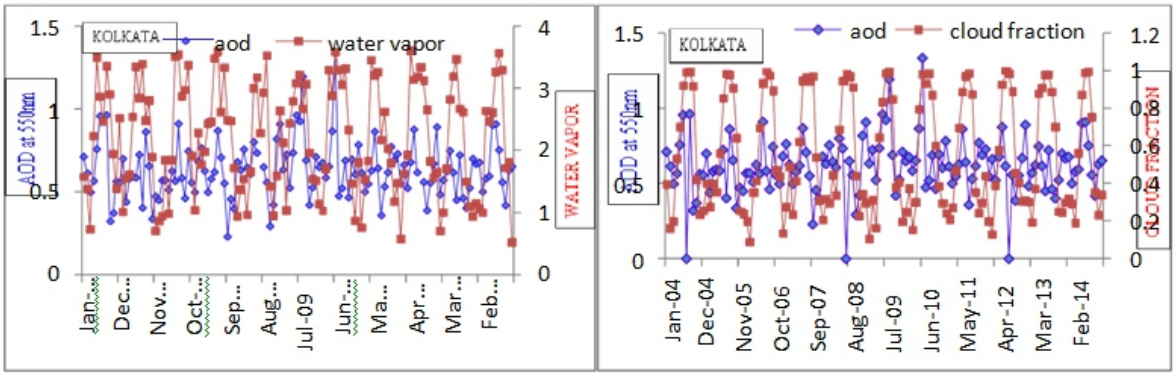

AOD VS WATER VAPOR **AOD VS CLOUD FRACTION**

Fig: 8(a) **Fig: 8(b)**

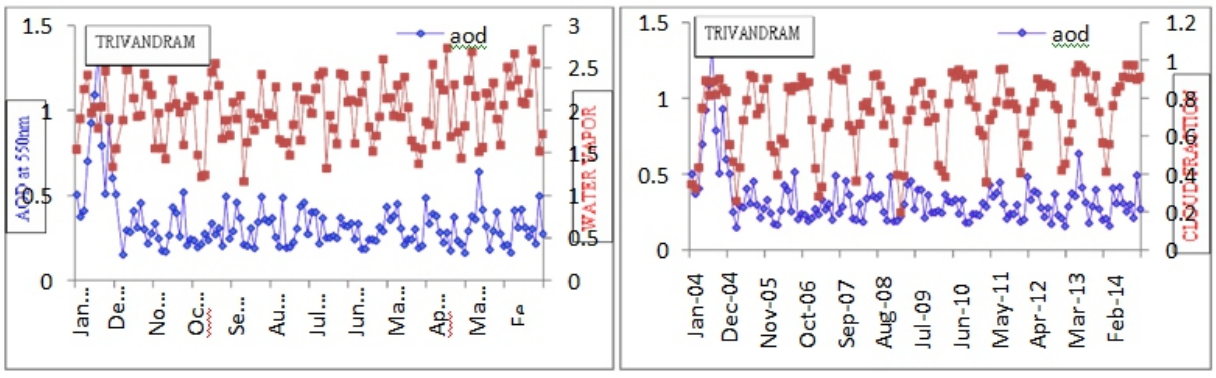

AOD VS WATER VAPOR **AOD VS CLOUD FRACTION**

Fig:8(c)

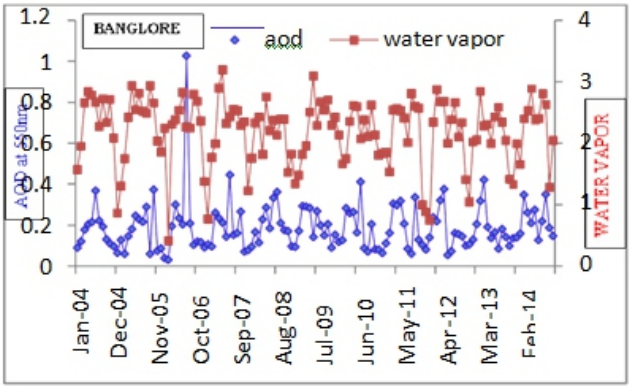

Fig:8(d)

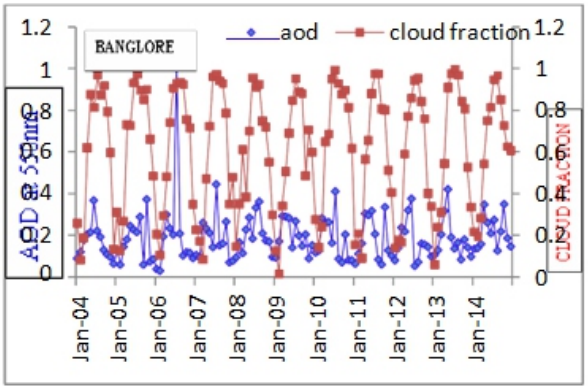

AOD VS WATER VAPOR

Fig:9(a)

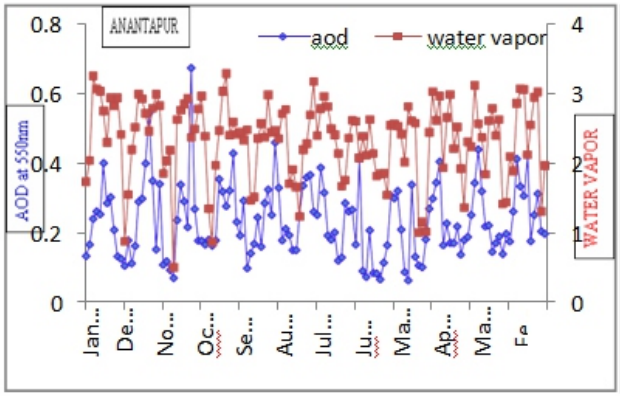

AOD VS CLOUD FRACTION

Fig:9(b)

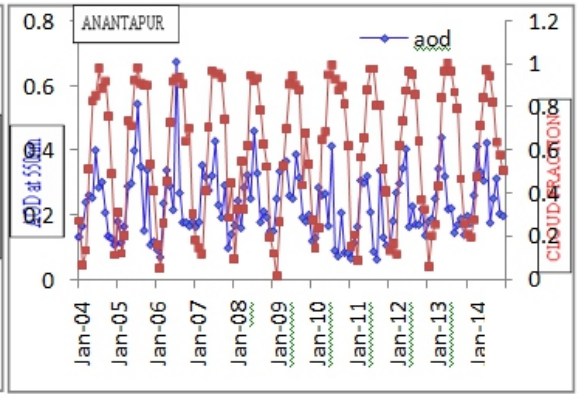

AOD VS WATER VAPOR

Fig:9(c)

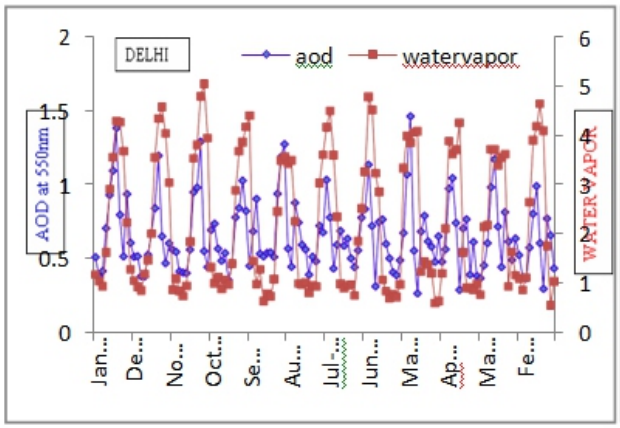

AOD VS CLOUD FRACTION

Fig:9(d)

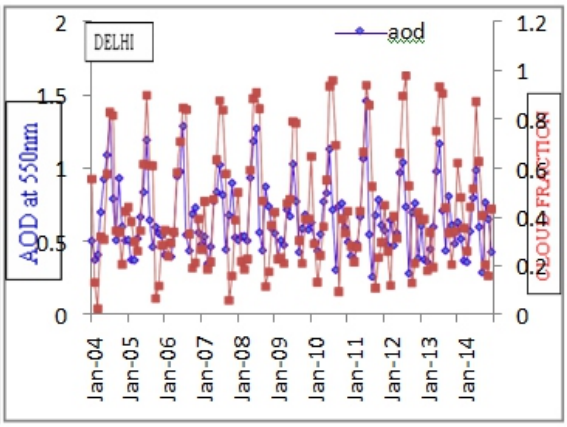

AOD VS WATER VAPOR

Fig:10(a)

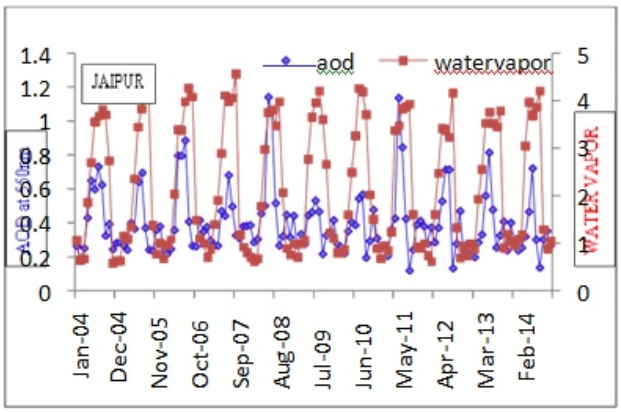

AOD VS CLOUD FRACTION

Fig:10(b)

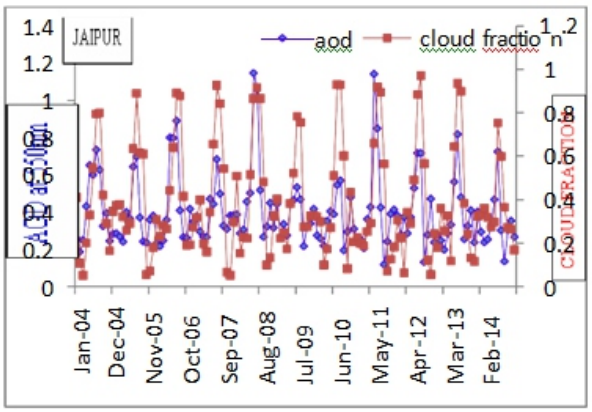

AOD VS WATER VAPOR

Fig:10(a)

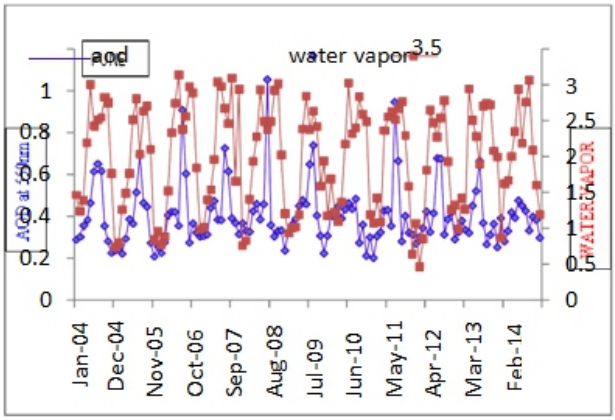

AOD VS CLOUD FRACTION

Fig:10(b)

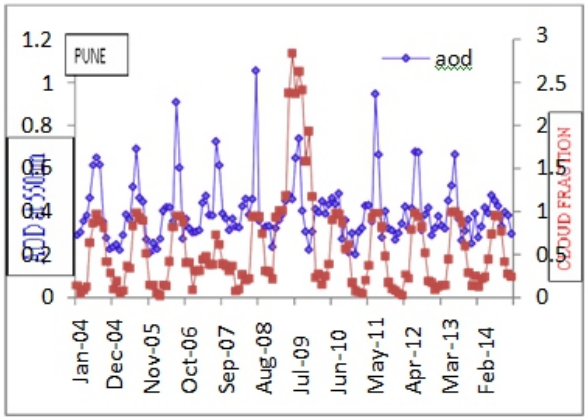

AOD VS WATER VAPOR

Fig:11(a)

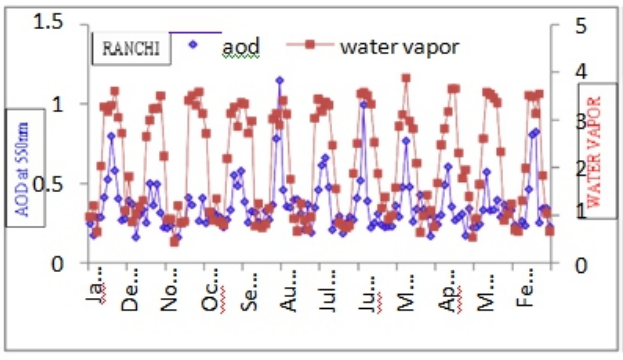

AOD VS CLOUD FRACTION

Fig:11(b)

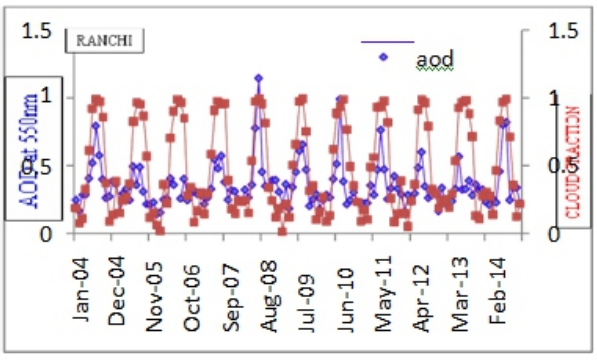

AOD VS WATER VAPOR

Fig:11(c)

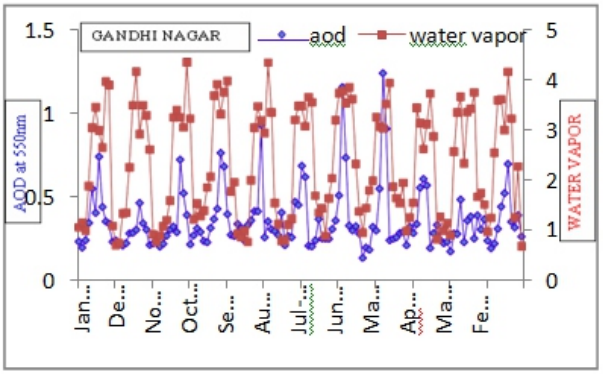

AOD VS CLOUD FRACTION

Fig:11(d)

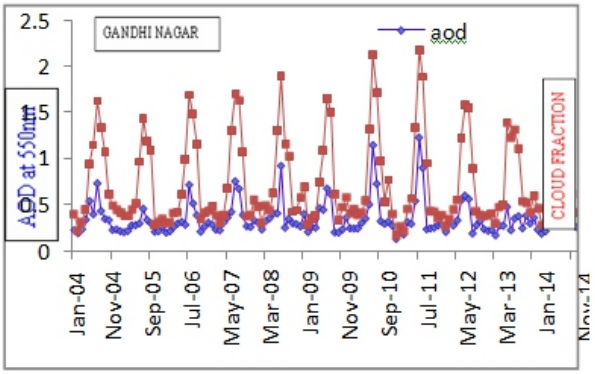

III. RESULTS AND DISCUSSIONS

Spatial distribution of annual mean aerosol optical depth:

The spatial distribution of annual mean aod at wave length of 550nm has been plotted for the period from 2004 to 2014 (Fig: 2). The fig: 2 shows that aerosols had marked impact on 10 cities in India namely Thiruvananthapuram, Banglore, Anantapur ,Pune, Visakhapatnam, Delhi, Ranchi, Jaipur, Kolkata, Gandhi Nagar. The spatial gradient of aod shows an increase from southern part of Indian sub-continent to northern part up to the Himalayas (Prasad et. al 2004). High aod values (> 0.4) are found over areas with intensive anthropogenic activity like the industrial region. The cloud fraction increases from western parts to eastern part (>0.3), where as the water vapor is maximum over land when compare to Himalayas.

SEASONAL VARIATIONS IN AOD:

Seasonal variations in aod were analyzed for the 10 selected cities and plotted in Fig: 5(a), (b), (c) and (d) respectively. The mean aod and standard deviation at 550nm were calculated for the above mentioned cities during the period 2004 to 2014. High mean aod values were observed in almost all regions during the summer season. High mean AOD values were observed during the summer season for the regions Jaipur and Delhi where as the low values are observed for the stations of Visakhapatnam, Kolkata and Anantapur. High AOD values were noticed during monsoon season of the stations Gandhi Nagar, Pune and Jaipur. The AOD values generally increase from lower latitude to higher latitude. AOD is found to be increasing rapidly in summer season that may cause adverse effect to the agricultural crop and also to the human health. Increased aerosol loading may likely affect the rainfall which is responsible for the observed drought conditions over the Indian sub-continent. The high AOD

values are noticed during the winter and post monsoon seasons for the stations Delhi, Gandhi Nagar and Pune when compared to the other stations. This can be attributed the fact that they are urban, Industrial and coastal station. Trivandrum, Anantapur have been noticed that low AOD values when compared to other cities in all seasons.

RELATIONSHIP BETWEEN AOD AND WATER VAPOR:

The changes in column water vapor in relation to aerosols are examined and this investigation gives an insight to understand the aerosol impact and the speed of the hydrological cycle (Myhre et al., 2007). The MODIS retrieval provides results for column water vapor in the clear sky and above cloud separately we used the above clouds data obtained from Terra for water vapor for the period between 2004 to 2014. The spatial correlation between AOD and water vapor shown in figure 6(a) reveals that AOD and water vapor have a stronger positive correlation at higher latitudes than at lower latitudes. The highest positive correlation (correlation coefficient 0.4,0.25, 0.1 and0.1) were found for Delhi, Jaipur, Gandhi Nagar and Pune, where as lower level of correlation was found for Anantapur and Banglore (-0.2). The time series plot for AOD and Water vapor also shows that these two parameters are increasing and decreasing simultaneously.

Relationship between AOD and Cloud Fraction: The satellite data show a strong correlation between total cloud fraction and AOD (Quass.et.al.,2009) Fig:6(b) shows the spatial correlation between AOD and cloud fraction for varies regions, MODIS shows an increase in the cloud fraction(CF) are cloud cover with increasing AOD in all areas. MODIS provides CF data for day time and night time, either separately; the combined data has been used for the present study. Correlation coefficience for AOD and cloud Fraction were also calculated for these 11 years. The correlation between AOD and Cloud fraction was found to be higher than that are coastal stations compared to continental. The correlation between AOD and CF was greater than 0.7 Gandhi Nagar, 0.5 in Visakhapatnam, 0.4 Jaipur and Pune and where as in Delhi, Anantapur, Ranchi and Trivandrum, it is (0.3, 0.3, 0.3 and 0.2) respectively. It is also important to mention between marked increase in the correlation between AOD with CF in those regions dominated by bio mass and dust aerosols, indicate in that meteorological factors influencing the relationship. Time series plots for spatial average of AOD and CF shows that CF increased with AOD at all location except for Kolkata (2004, 2008 and 2012) the values are in inverse condition. It shows in figure 7(d).

IV. SUMMARY AND CONCLUSIONS

The role of aerosols in modifying clouds and precipitation has been one of the most intriguing questions in cloud physics and to the study of climate change. Using MODIS satellite data, the spatial and temporal (seasonal) variability of aerosol has been investigated in order to develop an understanding of the impact of aerosols and cloud parameters. The spatial gradient of AOD shows an increase from southern part of Indian sub-continent to Northern part up to the Himalayas. High mean AOD values were observed during the summer season for the regions Jaipur and Delhi where as the low values are observed for the stations of Visakhapatnam, Kolkata and Anantapur. High AOD values were noticed during monsoon season of the stations Gandhi Nagar, Pune and Jaipur. The correlation between cloud fraction and AOD was found to be higher at coastal stations compared to continental. Cloud fraction was found to increase together with AOD in those regions dominated by biomass and dust aerosols, where as in regions dominated by marine and pollution aerosols there was good correlation between AOD and Cloud fraction. AOD, Water vapor and cloud fraction shown negative correlation for all the five stations over the south India and observed positive correlation in North India for the remaining five stations.

V. REFERENCES

1. Abbott, C. G., and F. E. Fowle, Jr., Annals of the Astrophysical Observatory of the Smithsonian Institution, Vol. II, Part 1, 11-124. US GPO, Washington, DC, 1908.

2. American Chemical Society, Chemistry in Context: Applying Chemistry to Society. 2000.

3. Bird, R., and C. Riordan, Simple Solar Spectral Model for Direct and Diffuse Irradiance on Horizontal and Tilted Planes at the Earth's Surface for Cloudless Atmosphere. Solar Energy Research Institute SERI/TR-215-2436, 1984. (online at rredc.nrel.gov/solar/pubs/spectral/model.)

4. Brooks, D. R., and F. M. Mims. III, Development of an inexpensive handheld LED-based Sun photometer for the GLOBE program. J. Geophys. Res. 106(D5), 4733-4740, 2001.

5. Brooks, David R., F. Niepold, G. D'Emilio, J. Glist, G. Hatterscheid, S. Martin, K. Dede, I. Neumann, Scientist-Teacher-Student Partnerships for Aerosol Optical Thickness Measurements in Support of Ground Validation Programs for Remote Sensing Spacecraft. 54th International Astronautical Congress, Bremen, Germany, Sept. 28 - Oct. 3, 2003.

6. Brooks, David R., Forrest M. Mims III, Arlene S. Levine, Dwayne Hinton, The GLOBE/GIFTS Water Vapor Monitoring Project:An Educator's Guide with Activities in Earth Sciences. NASA Publication EG- 2003-12-06-LARC, 2003.

7. Bucholtz, Anthony, Rayleigh-scattering calculations for the terrestrial atmosphere. Applied Optics, 34, 15, 2765-2773, 1995.

8. Diak, G. R., W. L. Bland, and J. R. Mecikalski, et al., A note on first estimates of surface insolation from GOES-8 visible satellite data. Agricultural and Forest Meteor. 82, 219-226, 1996. (See http://homer.ssec.wisc.edu/~insol/.).

9. Mims, Forrest M., III, Sun photometer with light-emitting diodes as spectrally selective detectors. Applied Optics, 31, 33, 6965-6967, 1992.

10. Mims, Forrest M. III, An inexpensive and stable LED Sun photometer for measuring the water vapor column over South Texas from 1990 to 2001, Geophys. Res. Lett., 29, 13, pp 20-1 -- 20-4, 2002.

Instructions for Authors

Essentials for Publishing in this Journal

1 Submitted articles should not have been previously published or be currently under consideration for publication elsewhere.

2 Conference papers may only be submitted if the paper has been completely re-written (taken to mean more than 50%) and the author has cleared any necessary permission with the copyright owner if it has been previously copyrighted.

3 All our articles are refereed through a double-blind process.

4 All authors must declare they have read and agreed to the content of the submitted article and must sign a declaration correspond to the originality of the article.

Submission Process

All articles for this journal must be submitted using our online submissions system. http://enrichedpub.com/ . Please use the Submit Your Article link in the Author Service area.

Manuscript Guidelines

The instructions to authors about the article preparation for publication in the Manuscripts are submitted online, through the e-Ur (Electronic editing) system, developed by **Enriched Publications Pvt. Ltd**. The article should contain the abstract with keywords, introduction, body, conclusion, references and the summary in English language (without heading and subheading enumeration). The article length should not exceed 16 pages of A4 paper format.

Title

The title should be informative. It is in both Journal's and author's best interest to use terms suitable. For indexing and word search. If there are no such terms in the title, the author is strongly advised to add a subtitle. The title should be given in English as well. The titles precede the abstract and the summary in an appropriate language.

Letterhead Title

The letterhead title is given at a top of each page for easier identification of article copies in an Electronic form in particular. It contains the author's surname and first name initial .article title, journal title and collation (year, volume, and issue, first and last page). The journal and article titles can be given in a shortened form.

Author's Name

Full name(s) of author(s) should be used. It is advisable to give the middle initial. Names are given in their original form.

Contact Details

The postal address or the e-mail address of the author (usually of the first one if there are more Authors) is given in the footnote at the bottom of the first page.

Type of Articles

Classification of articles is a duty of the editorial staff and is of special importance. Referees and the members of the editorial staff, or section editors, can propose a category, but the editor-in-chief has the sole responsibility for their classification. Journal articles are classified as follows:

Scientific articles:

1. Original scientific paper (giving the previously unpublished results of the author's own research based on management methods).

2. Survey paper (giving an original, detailed and critical view of a research problem or an area to which the author has made a contribution visible through his self-citation);

3. Short or preliminary communication (original management paper of full format but of a smaller extent or of a preliminary character);

4. Scientific critique or forum (discussion on a particular scientific topic, based exclusively on management argumentation) and commentaries. Exceptionally, in particular areas, a scientific paper in the Journal can be in a form of a monograph or a critical edition of scientific data (historical, archival, lexicographic, bibliographic, data survey, etc.) which were unknown or hardly accessible for scientific research.

Professional articles:

1. Professional paper (contribution offering experience useful for improvement of professional practice but not necessarily based on scientific methods);
2. Informative contribution (editorial, commentary, etc.);
3. Review (of a book, software, case study, scientific event, etc.)

Language

The article should be in English. The grammar and style of the article should be of good quality. The systematized text should be without abbreviations (except standard ones). All measurements must be in SI units. The sequence of formulae is denoted in Arabic numerals in parentheses on the right-hand side.

Abstract and Summary

An abstract is a concise informative presentation of the article content for fast and accurate Evaluation of its relevance. It is both in the Editorial Office's and the author's best interest for an abstract to contain terms often used for indexing and article search. The abstract describes the purpose of the study and the methods, outlines the findings and state the conclusions. A 100- to 250- Word abstract should be placed between the title and the keywords with the body text to follow. Besides an abstract are advised to have a summary in English, at the end of the article, after the Reference list. The summary should be structured and long up to 1/10 of the article length (it is more extensive than the abstract).

Keywords

Keywords are terms or phrases showing adequately the article content for indexing and search purposes. They should be allocated heaving in mind widely accepted international sources (index, dictionary or thesaurus), such as the Web of Science keyword list for science in general. The higher their usage frequency is the better. Up to 10 keywords immediately follow the abstract and the summary, in respective languages.

Acknowledgements

The name and the number of the project or programmed within which the article was realized is given in a separate note at the bottom of the first page together with the name of the institution which financially supported the project or programmed.

Tables and Illustrations

All the captions should be in the original language as well as in English, together with the texts in illustrations if possible. Tables are typed in the same style as the text and are denoted by numerals at the top. Photographs and drawings, placed appropriately in the text, should be clear, precise and suitable for reproduction. Drawings should be created in Word or Corel.

Citation in the Text

Citation in the text must be uniform. When citing references in the text, use the reference number set in square brackets from the Reference list at the end of the article.

Footnotes

Footnotes are given at the bottom of the page with the text they refer to. They can contain less relevant details, additional explanations or used sources (e.g. scientific material, manuals). They cannot replace the cited literature.
The article should be accompanied with a cover letter with the information about the author(s): surname, middle initial, first name, and citizen personal number, rank, title, e-mail address, and affiliation address, home address including municipality, phone number in the office and at home (or a mobile phone number). The cover letter should state the type of the article and tell which illustrations are original and which are not.

Address of the Editorial Office:

Enriched Publications Pvt. Ltd.
S-9,IInd FLOOR, MLU POCKET,
MANISH ABHINAV PLAZA-II, ABOVE FEDERAL BANK,
PLOT NO-5, SECTOR -5, DWARKA, NEW DELHI, INDIA-110075,
PHONE: - + (91)-(11)-45525005